

ESD ACCESSION LIST

TRI Call No. 75827
 Copy No. 1 of 1 cys.

TRI FILE COPY

Technical Report

490

ELF Noise Processing

A. S. Griffiths

ESD RECORD COPY

RETURN TO
 SCIENTIFIC & TECHNICAL INFORMATION DIVISION
 (TRI), Building 1210

13 January 1972

Prepared for the Department of the Navy
 under Electronic Systems Division Contract F19628-70-C-0230 by

Lincoln Laboratory

MASSACHUSETTS INSTITUTE OF TECHNOLOGY

Lexington, Massachusetts



AD739907

Approved for public release; distribution unlimited.

MASSACHUSETTS INSTITUTE OF TECHNOLOGY
LINCOLN LABORATORY

ELF NOISE PROCESSING

A. S. GRIFFITHS

Group 66

TECHNICAL REPORT 490

13 JANUARY 1972

Approved for public release; distribution unlimited.

The work reported in this document was performed at Lincoln Laboratory, a center for research operated by Massachusetts Institute of Technology. The work was sponsored by the Department of the Navy under Air Force Contract F19628-70-C-0230.

This report may be reproduced to satisfy needs of U.S. Government agencies.

Non-Lincoln Recipients

PLEASE DO NOT RETURN

Permission is given to destroy this document
when it is no longer needed.

ABSTRACT

This report describes noise processing experiments with ELF (3 to 300 Hz) atmospheric noise and signals in the 40- to 80-Hz range. The primary purpose of the experiments was to design the noise processing portion of a submarine-borne receiver which would minimize the required transmitter power of the Sanguine communications system. The recommended noise processor included a nonlinearity followed by a matched filter and consisted of the following functions: (1) a compensating (or whitening) filter, (2) a pre-notch filter clipper, (3) notch filters at power line frequencies, (4) a post-notch filter clipper, and (5) a phase-coherent linear matched filter.

For linear receivers, the output signal-to-noise ratio depends only upon the received signal energy and the noise power spectral density (or spectral level) at the signal frequency. For nonlinear receivers, an effective noise level (twice the received signal energy divided by the matched filter output signal-to-noise ratio) has been used to measure system performance and is convenient for system sizing calculations. Simulations on a digital computer using recorded ELF noise indicate that nonlinear processing provides considerable gain relative to linear processing. For example, using clippers, the highest effective noise levels observed at 45 Hz were about -134, -131, and -137 dB wrt 1 amp/m $\sqrt{\text{Hz}}$ using Saipan, Malta, and Norway data, respectively, compared to 1 percent exceedance spectral levels of about -115, -115, and -130 dB wrt 1 amp/m $\sqrt{\text{Hz}}$, respectively.

Simulations were conducted to determine the sensitivity of processing gains to several parameters. Effective noise levels using signal frequencies in the 75- to 80-Hz range were consistently 3 to 4 dB lower than comparable levels using signal frequencies between 40 and 45 Hz. Clippers performed nearly as well as more complicated forms of nonlinear processing and, in general, displayed less sensitivity to parameter settings and receiver gains. Hard limiters typically provided effective noise levels 0.5 to 1.5 dB higher than clippers with optimal clip levels. Effective noise levels were relatively insensitive to the characteristics of the compensating filter whose bandwidth could be reduced from 300 to 150 Hz with reductions in processing gain of less than 1 dB. Experiments using clippers at simulated antenna depths of 75 to 200 meters and submarine speeds of 8 to 14 knots indicated that the resultant effective noise levels including antenna noise could be approximated by adding the effective levels observed in the absence of antenna noise to antenna noise spectral levels at the signal frequency.

Accepted for the Air Force
Joseph R. Waterman, Lt. Col., USAF
Chief, Lincoln Laboratory Project Office

CONTENTS

Abstract	iii
Symbols and Abbreviations	vi
I. INTRODUCTION	1
II. EXPERIMENTAL PROCEDURE	2
III. SUMMARY OF NOISE CHARACTERISTICS	5
A. Florida Noise	7
B. Saipan Noise	7
C. Malta Noise	9
D. Norway Noise	11
E. ELF Noise Model	11
F. Antenna Noise	13
IV. PROCESSING SENSITIVITY TO COMPENSATING FILTER CHARACTERISTICS	14
V. PROCESSING SENSITIVITY TO NONLINEARITY CHARACTERISTICS	15
VI. EFFECTIVE NOISE LEVEL SENSITIVITY TO INPUT SPECTRAL LEVELS	19
VII. PROCESSING SENSITIVITY OF SIGNAL FREQUENCY	19
VIII. PROCESSING SENSITIVITY TO SIGNAL LEVEL	20
IX. PROCESSING AT DEPTH	21
A. Theoretical Estimate of Antenna Noise Effects	23
B. Experiments with Simulated Antenna Noise at Depth	25
X. PROCESSING SENSITIVITY TO INTERFERENCE	26
A. Notch Filtering	29
XI. CONCLUSIONS	32
APPENDIX A - Two-Sensor Processing of ELF Noise	35
APPENDIX B - Processing Sensitivity to Sample Rate	37
References	39

SYMBOLS AND ABBREVIATIONS

<u>Symbol or Abbreviation</u>	<u>Definition</u>
APD	amplitude probability density
dBH	H-field (dB wrt 1 amp/m)
dBH _O	H-field spectral density (dB wrt 1 amp/m $\sqrt{\text{Hz}}$)
E _S	signal energy per matched filter integration period
H _S	received signal H-field (amp/m)
HL	hard limiter
k _p	duty factor of pulse process
LIN	linear
MSK	minimum frequency shift modulation
N _{eff}	effective noise level = $2H_S^2 T_S / \text{SNR}$
N _O	single-sided noise power spectral density (spectral level)
NL	nonlinear
p(x)	amplitude probability density function
SNR	matched filter output signal-to-noise ratio (mean ² /variance)
T _c	duration of one MSK chip
T _S	signal integration time of matched filter
wrt	with respect to

ELF NOISE PROCESSING

I. INTRODUCTION

This document with its companion reports¹⁻⁵ describes analytical and experimental work at Lincoln Laboratory on the design and analysis of an ELF communications receiver. Key elements of the communications system are (a) minimum frequency shift keying⁶ (MSK) modulation to minimize signal bandwidth requirements, (b) sequential decoding to minimize required signal-to-noise ratios, (c) phase tracking to allow coherent matched filtering, and (d) nonlinear processing to minimize the effects of atmospheric noise. This report describes the design and analysis of the noise processing portion of the receiver.

The dominant source of noise in the ELF band is attributed to radiation induced by lightning.^{7,8} Since there is a worldwide variation in thunderstorm activity, there is a corresponding variation throughout the world in ELF noise characteristics. Due to the low attenuation rate⁹ which makes long-range communications possible in this band, noise characteristics are affected not only by local storms but also by storms thousands of miles away. The effect of local storms is to produce large spikes, illustrated by the waveform of Fig. 1, while the effect of distant storms is a background noise with occasional spikes.

An important aspect of ELF noise is its distinctly non-Gaussian character. Analysis of data recorded in Norway indicates that even in quiet regions, far from storm centers, ELF noise is non-Gaussian. A typical amplitude probability density (APD), shown by Fig. 2, has

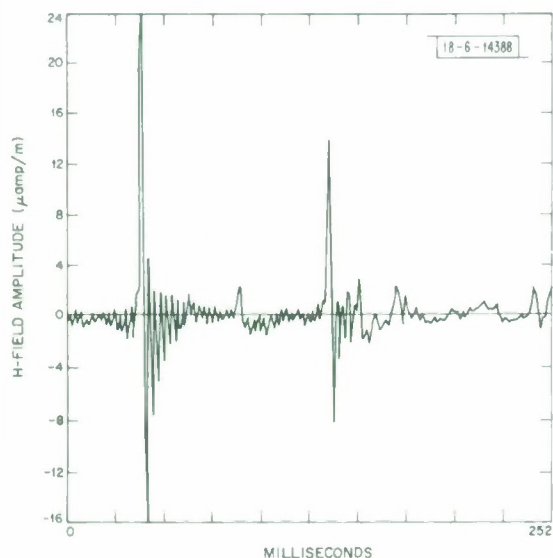


Fig. 1. Typical waveform of high-level ELF noise.

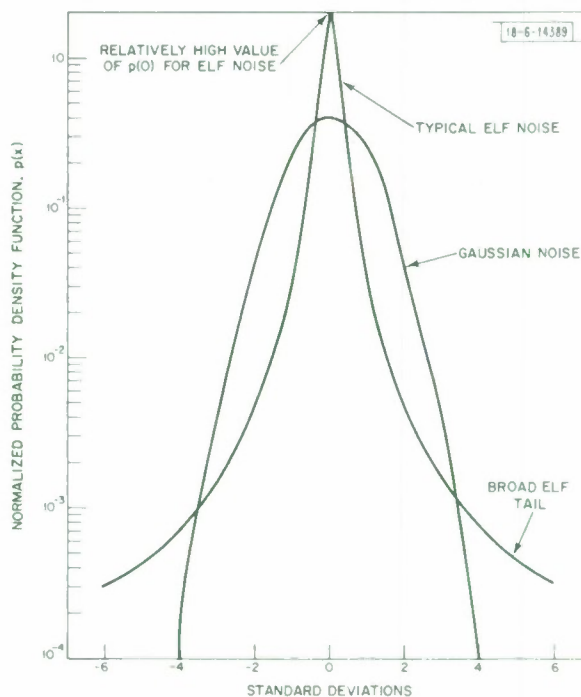


Fig. 2. Normalized amplitude probability density of Gaussian noise and ELF noise.

relatively broad tails and high values at the origin compared to Gaussian noise. While linear receivers are optimum in a Gaussian noise environment,¹⁰ more sophisticated techniques are required to optimize receiver performance in a non-Gaussian noise environment.

In a non-Gaussian environment, the design of an optimum receiver requires a detailed analytical model of the noise process. Computer analysis of wideband recordings from Saipan, Malta, and Norway indicates that APD's, waveforms, and first-order statistics can be matched by using a model consisting of the sum of a Gaussian background process (attributed to many distant thunderstorms) and a filtered Poisson impulse process (attributed to local lightning activity).⁴ From such a model one can derive an optimum receiver configuration⁵ which would form estimates of the impulsive noise component and the signal component and which would use these estimates as a reference for correlation. Because of this complexity, a simpler nonlinear processor has been proposed. Based upon analysis of measured APD's, the performance of a processor which clips or suppresses the input when spikes are present should be close to the optimum receiver. The performance of the optimum receiver is limited by the Gaussian background plus some residue due to pulse estimation errors; the performance of a clipper or hole puncher is similarly limited by the Gaussian noise when pulses are absent but suffers a further degradation due to capture or blanking when the pulses are present. If the duty factor of the pulses is small, as analysis of available recordings indicates,⁴ this degradation will be small.

The motivation for examining a nonlinearity (such as a clipper or hole puncher) followed by a matched filter comes from examining sampled data receiver structures. If one assumes independent noise samples (and low level signals), optimum receiver structures can be derived as a nonlinearity followed by a matched filter.^{11,12} Preceding the clipper, a filter is used to compensate for time smearing of the pulses by the atmospheric and ocean channel and to thereby restore the impulse-like property of the lightning strokes. Notch filters are used to reduce power line interference which otherwise can "capture" the clipper. To reduce prolonged ringing at the narrowband notched filter output, a pre-notch clipper is used to clip the large spikes.

Subsequent sections of this report describe experiments designed to select parameters of the nonlinear processing and to determine required received signal strength. Specifically, the following sections are entitled:

- II. Experimental Procedure
- III. Summary of Noise Characteristics
- IV. Processing Sensitivity to Compensating Filter Characteristics
- V. Processing Sensitivity to Nonlinearity Characteristics
- VI. Effective Noise Level Sensitivity to Input Spectral Levels
- VII. Processing Sensitivity of Signal Frequency
- VIII. Processing Sensitivity to Signal Level
- IX. Processing at Depth
- X. Processing Sensitivity to Interference
- XI. Conclusions

II. EXPERIMENTAL PROCEDURE

To provide data for analysis and simulations, wideband (approximately 10 to 350 Hz) recordings were made in Malta (Winter 1968-1969), Norway (Winter, Spring, Summer 1969) and Saipan (Summer, Fall 1969). These recording areas had been chosen to represent typical operating environments for the Sanguine receivers. A limited number of analog recordings were also taken in Florida and New Hampshire. Sites were chosen as far away from power line

interference as possible, although 50-Hz, 150-Hz, and 250-Hz interference was pronounced in Norway and Malta. Saipan data had much lower interference levels. Approximately 140 tapes were recorded in Norway, 200 in Malta, and 160 in Saipan, using three sensors: a whip antenna and two orthogonally oriented vertical loop antennas. Recordings were made at various times of day under a variety of weather conditions. At Malta, a concerted effort was made to obtain several recordings during local thunderstorms.

The tapes were first analyzed on an IBM 360/67. Spectral analysis using 1 to 5 minutes of data was performed on each tape both to check the validity of the data and to classify tapes according to their spectral levels for subsequent analysis. Calibration was also obtained by spectral analysis, measuring the spectral level of a 100-Hz sine wave which was injected at the antenna outputs. APD's and burst statistics were computed for several tapes from each recording site. Many tapes were processed using an ELF receiver simulated first in FORTRAN on the IBM 360/67 and then on the simulation facility.²

Several factors indicated that a great amount of noise data should be analyzed. First, worst case conditions should be found and examined to compare system performance to the stringent low error rate requirements.¹³ Second, due to message lengths of several minutes and the non-stationarity of ELF noise, several minutes of data are required for any meaningful measurement. Third, because ELF noise characteristics vary greatly in different parts of the world, several areas had to be examined. Fourth, several parameters such as signal frequency and nonlinearity characteristics had to be examined. Finally, accurate measures of system performance were important since a 1-dB change of required transmitter power corresponds to millions of estimated cost change.¹³ Even with several hundred ELF recordings available, statistical analysis of worst case conditions was therefore impossible.* Furthermore, practical limitations of computer time restricted the amount of data that could be analyzed.

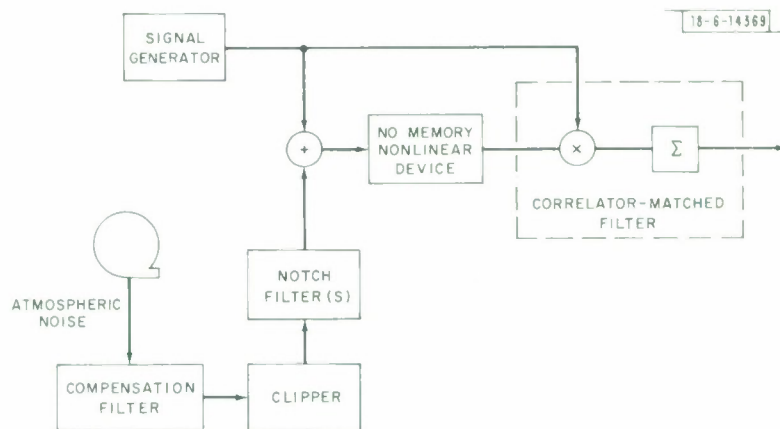


Fig. 3. Simplified simulated receiver without phase tracking.

Several steps were taken to minimize computer processing time. A simplified and hence faster simulated receiver without phase tracking or decoding was used initially as shown by Fig. 3. Relatively short message lengths were often used. In search for worst case conditions, simulations with high-level input noise were emphasized, assuming that high effective noise levels might correspond to high input spectral levels.

* Lincoln Laboratory is conducting a series of field measurements with on-site nonlinear processing to provide more data.

Analysis of the wideband recordings involved several steps.

- (a) Selection and filtering of segments of noise data using an FFT (fast Fourier transform) filter program on the 360 facility. The high and low gain channels of each loop antenna (corresponding to the time derivative of the H-field) were combined and filtered to give two channels (north-south and east-west) which were recorded on magnetic tape.
- (b) Spectral analysis (using an FFT 360 program) providing graphic outputs.
- (c) Preliminary simulation on the 360 using an injected sine wave signal of known phase and amplitude, providing matched filter output statistics and plots of output distributions.
- (d) Conversion of digital tape to format compatible with the receiver simulation programs^{2,3} on a Varian 620/i computer.
- (e) Repeated simulations with several parameter variations using receiver programs with injected sine wave signal of known amplitude and phase, providing matched filter output statistics and plots of outputs vs time.
- (f) Confirmation of test results using MSK waveforms and phase tracking on the simulated receiver.

Simulations with nonlinear processing consistently yielded matched filter outputs which followed a Gaussian distribution as illustrated by Fig. 4. Moreover, simulations using symbol interleaving¹ to minimize the effects of burst noise indicated that the matched filter outputs

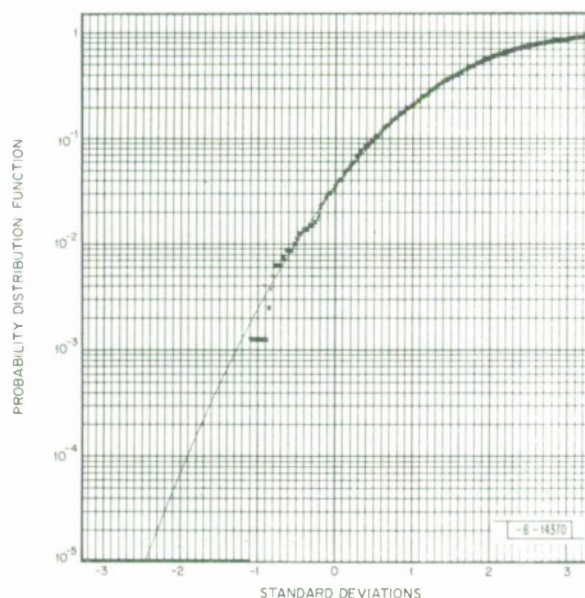


Fig. 4. Typical APD of matched filter outputs using nonlinear processing. Smooth curve represents probability distribution for Gaussian process with the same mean and variance.

were nearly independent. One parameter, the signal-to-noise ratio at the matched filter output, could therefore describe the matched filter outputs¹⁰ and hence the performance of the noise processor. Furthermore, the noise processor and the sequential decoder could then be tested independently,⁸ thereby greatly reducing computer processing time.

*Simulations with the sequential decoder comparing independent Gaussian samples to actual matched filter outputs indicated that there was a slight correlation in the matched filter outputs resulting in less than $\frac{1}{4}$ -dB increase in required signal-to-noise ratio.¹⁴

In contrast to a linear matched filter receiver where the signal-to-noise ratio (mean²/variance) is¹⁰

$$\text{SNR}_{\text{LIN}} = \frac{2E_s}{N_o}, \quad (1)$$

where

E_s = signal energy,

N_o = single-sided noise power spectral density,

nonlinear processing yields output signal-to-noise ratios which are not directly related to the noise spectrum level, N_o . It has therefore been convenient in describing the effects of ELF noise to define an effective H-field spectrum level:

$$N_{\text{eff}} \triangleq \frac{2H_s^2 T_s}{\text{SNR}_{\text{NL}}}, \quad (2)$$

where

SNR_{NL} = signal-to-noise ratio at nonlinear processor output (including matched filter),

H_s = received signal H-field (amp/m),

T_s = matched filter integration time.

The unit of measure used in this report for the effective noise level is dB wrt 1 amp/m $\sqrt{\text{Hz}}$, which has been abbreviated dBH_o, corresponding to the H-field spectral density.* Similarly, signal power or power line interference levels have been expressed in dB wrt 1 amp/m, abbreviated dBH, corresponding to the H-field power. For operation at depth, where both the atmospheric noise and signal levels are attenuated by the ocean channel, effective noise levels are expressed in equivalent levels at the surface to avoid subsequent computation of ocean channel losses. Similarly, receiver clip levels at depth are expressed as H-field measurements at the surface.

III. SUMMARY OF NOISE CHARACTERISTICS

The predominant source of noise in the ELF band is thunderstorm activity. Due to the low attenuation rate particularly at the lower frequencies, the noise in any location is affected by activity thousands of miles away. The areas with the highest noise are those close to the great storm centers of the world - Central Africa, South America, and the South Pacific.¹⁵ Among the quietest areas are the polar regions where local thunder activity is extremely rare.

Geographic, seasonal, and diurnal variations in ELF noise levels can be obtained from narrowband spectral measurements.^{16,17} However, to determine the effect of nonlinear processing, wideband analysis is necessary. Following is a summary of the wideband characteristics observed from recordings made in Florida, Saipan, Malta, and Norway. Also summarized are an ELF noise model developed from analysis of these recordings and a description of antenna noise.

* The E-field spectral density in dB wrt volt/m $\sqrt{\text{Hz}}$ can be obtained by adding $20 \log z$ (where z is the impedance of the medium) to the H-field measured in dBH. For free space, $20 \log z_o = 20 \log 377 = 51.5 \text{ dB}$.

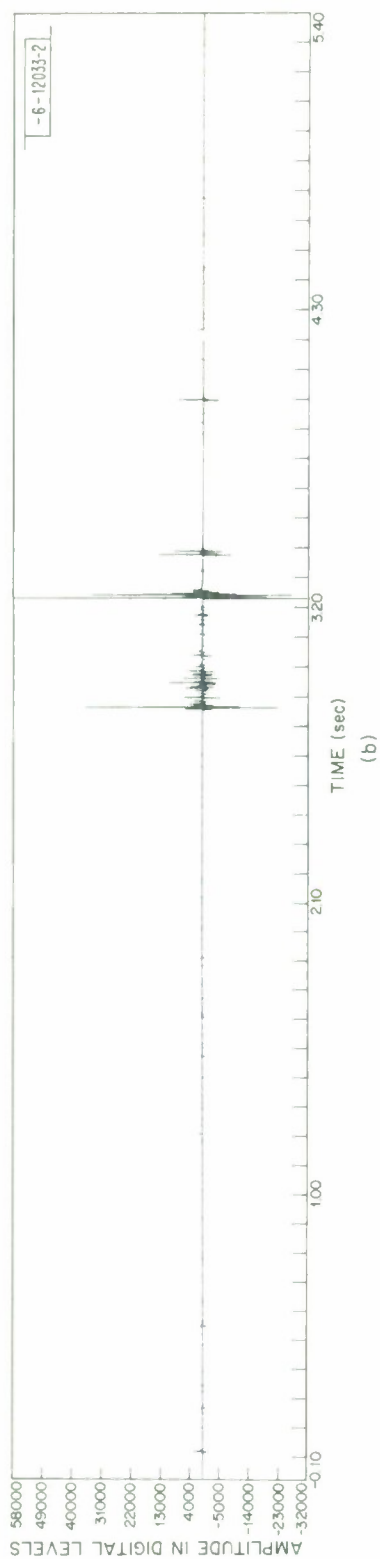
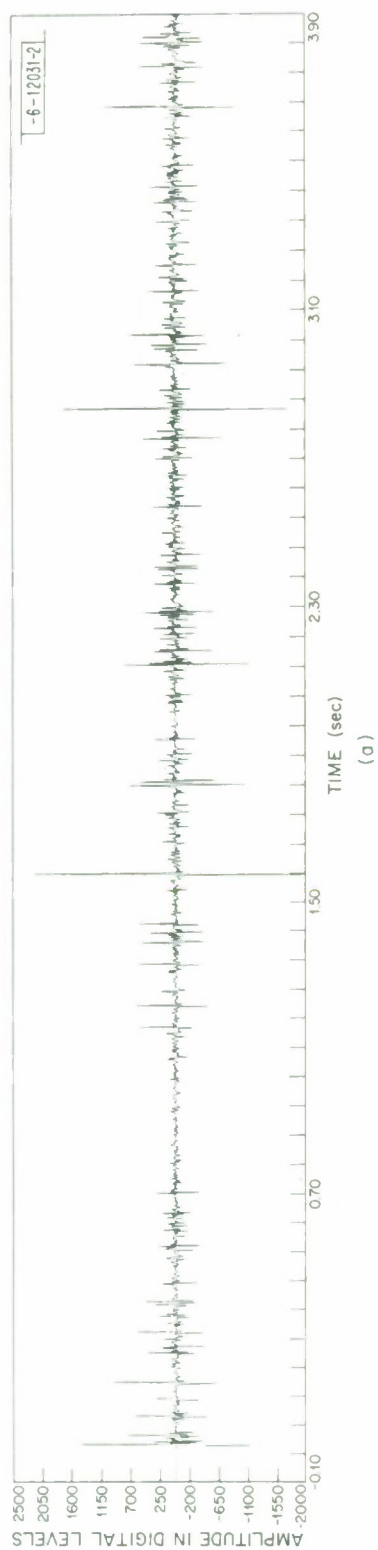


Fig. 5. Typical wideband waveforms recorded in Saipan: (a) median-level; (b) high-level.

A. Florida Noise

Although the Florida recordings did not represent noise from Sanguine operational areas, they did provide a valuable equipment check and a point of comparison for other ELF noise recordings. Analysis of the Florida data has been documented in an earlier report⁷ which also includes preliminary descriptions of Malta recordings. In summary, the wideband Florida noise exhibited distinctly non-Gaussian characteristics. High-level noise was characterized by frequent (several per second) spikes which were well above the background. Moreover, the process seemed stationary over half-hour periods.

B. Saipan Noise

Although the median spectral levels for the Saipan and Florida recordings were similar, the high-level noise from these locations differed markedly. High noise levels in Saipan arise when infrequent, but extremely large, spikes are received. Figures 5(a) and (b) show waveforms of the Saipan data corresponding to median and very high spectrum levels. The very large, but infrequent, spikes that occurred when the spectrum level was high presumably are generated by a single or very small number of local storms in contrast to the Florida high noise levels which seemed to arise from a large number of somewhat smaller spikes. Wideband spectral analysis of high-level Saipan noise also illustrated the effect of infrequent but powerful spikes in time. The oscillations shown in Fig. 6 indicate an interference pattern of a few closely spaced pulses which dominate the spectral measurements averaged over several minutes of data.

The temporal distribution of power over the 5-minute period used to obtain the Saipan spectra was also quite different from the Florida data. Figure 7 shows the time variation in power from 35 to 45 Hz for Florida data having approximately equal spectrum levels. It is clear from Fig. 7 that the rate of noise energy arrival in Saipan is much less constant than that in Florida.

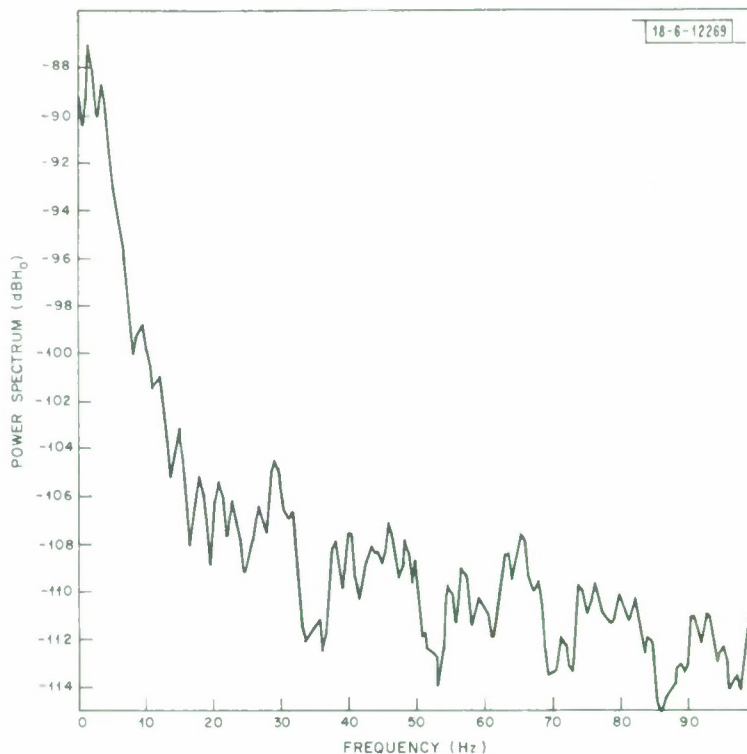


Fig. 6. Spectrum of high-level Saipan noise.

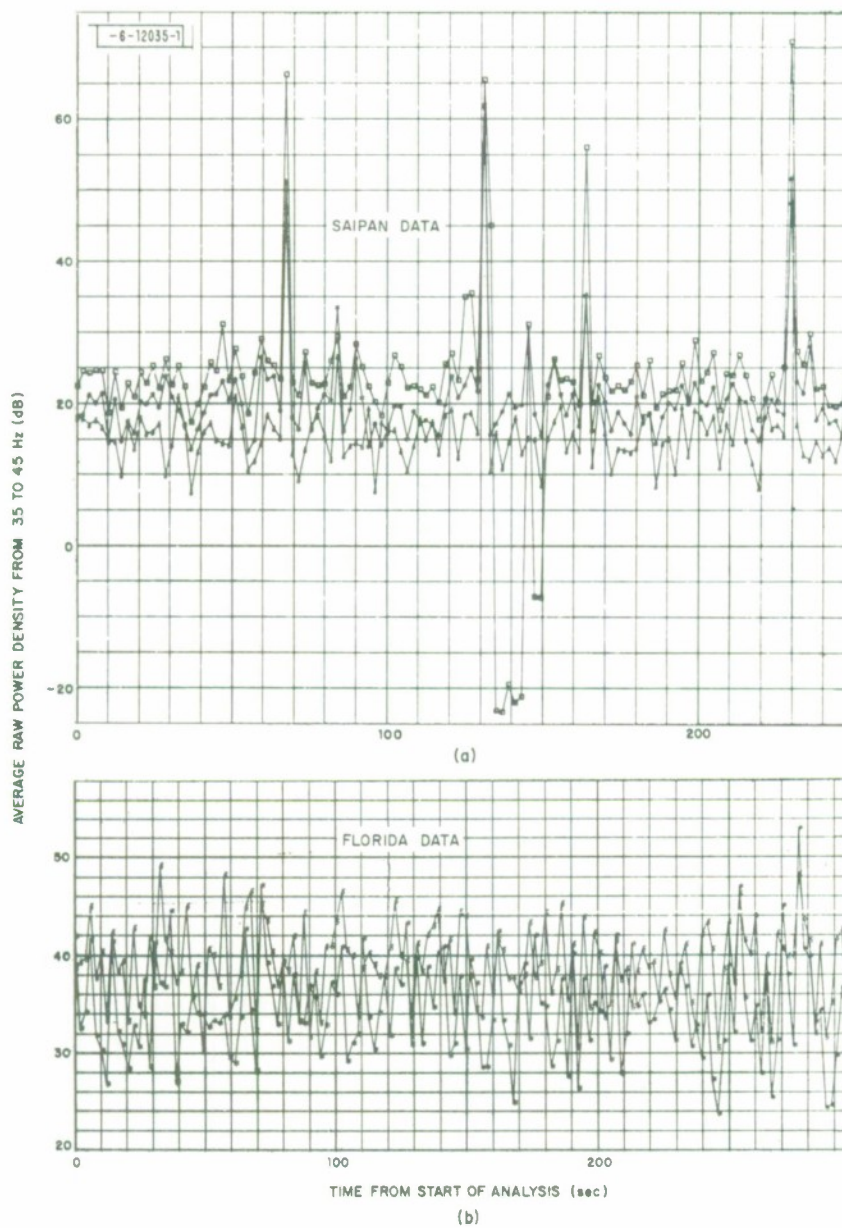
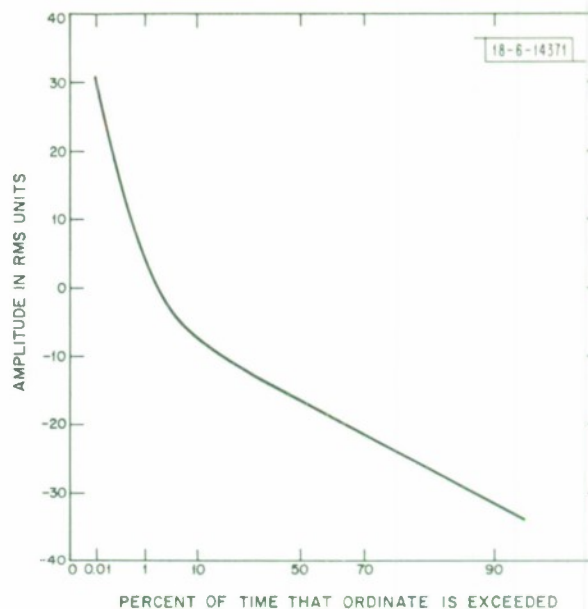


Fig. 7. Time variation of ELF power: (a) Saipan; (b) Florida.

Fig. 8. APD of high-level Saipan H-field ELF noise.



The very large, but infrequent, spikes that are characteristic of the high-level Saipan data are also reflected in the APD of the data. Figure 8, the exceedance probability as a function of normalized noise amplitude for various Saipan and Florida data, illustrates that the high-level Saipan data are small relative to the (wideband) rms level a much greater fraction of the time than are the Florida data, Saipan median noise, or Gaussian noise. However, the Saipan high-level noise APD has a tail that drops considerably slower than the tails of the other noise data.

C. Malta Noise

The most striking observation from analysis of Malta data is that high-level noise is characterized by short very high-level bursts between which the background level is not much greater than median. Like the Saipan data, all the high levels observed from the Malta recordings (greater than -122 dBH_0) were caused by few bursts less than 2 seconds in duration. Spectral levels averaged over 2 minutes of data can be raised by 5 to 30 dB by a single burst. Figure 9, a time plot of successive spectral measurements (each corresponding to 2 seconds of data), over a period of 250 seconds, illustrates the sudden changes in spectral level observed during stormy periods. At $t = 136$ seconds, the level on the north-south channel jumped about 40 dB above the background, and on the east-west channel about 35 dB above the background, raising the average for the 2-minute interval by 22 and 17 dB, respectively. With these short bursts, the spectral levels at 45 Hz were -111 and -116 dBH_0 ; without them the noise levels would have been below the median. Such occurrences are typical of the high-level noise observed in Malta.

Shown in Fig. 10 is a typical 4-minute segment of median-level noise. Although the background is about the same level as that shown in Fig. 9, the absence of spikes much larger than 30 dB above the background results in an average spectral level of about -126 dBH_0 , close to the median level. Quiet periods with spectral levels below -130 dBH_0 typically had peak levels no greater than 5 dB above the median level, while noisy tapes above -122 dBH_0 typically had one or two pulses 25 to 50 dB above the median level. Even during these noisy periods, the background level was not increased by more than 2 or 3 dB.

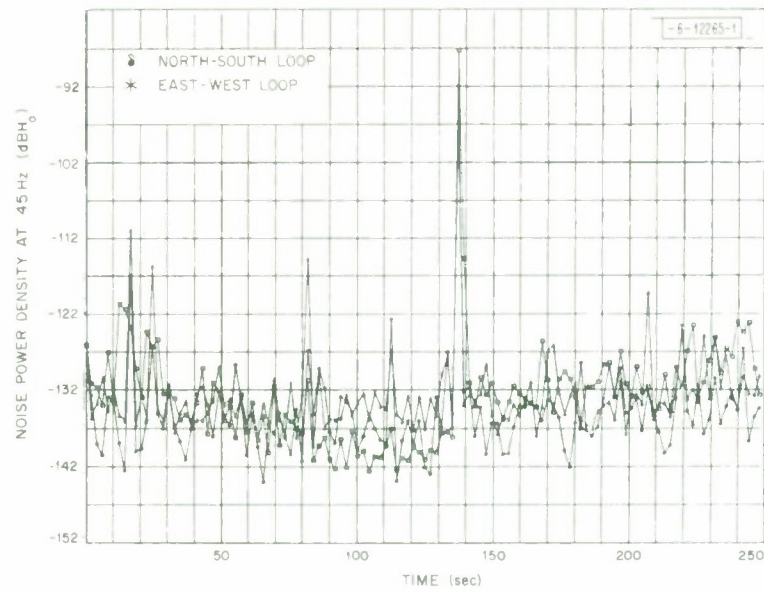


Fig. 9. Time variation of ELF power for high-level Malta noise.

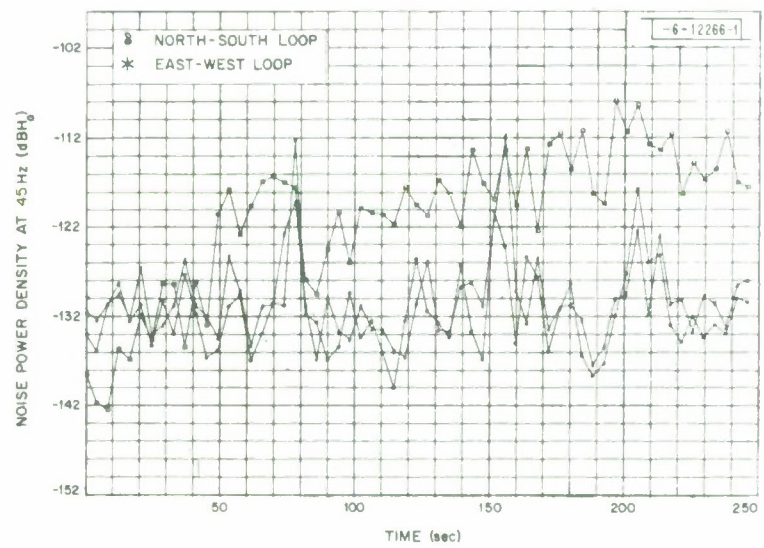


Fig. 10. Time variation of ELF power for median-level Malta noise.

Figure 11 shows a typical spectrum obtained from median-level Malta recordings with a system bandwidth of about 350 Hz. On east-west loop recordings, 50-Hz power line interference and its third harmonic (despite a 150-Hz notch filter) were 10 to 25 dB above the background when measured with a frequency resolution of 0.5 Hz; power line pickup on the north-south loop was 5 to 15 dB lower. In contrast to the slight statistical fluctuations of the median-level data, high-level noise is characterized by significantly greater fluctuations in the spectrum as shown by Fig. 12, suggesting that the interference pattern of a few big pulses with the same 2-second interval dominates the 2-minute spectral average. There appeared to be no consistent pattern in spectral fluctuations observed, implying no consistent pattern in the spacings of the big pulses.

D. Norway Noise

Unlike Florida, Saipan, and Malta, local thunderstorms in Norway are a rarity. Consequently, the characteristics of Norway ELF noise did not change much during a single half-hour recording or from day to day. The observed spectrum levels varied only ± 5 dB compared to ± 15 dB observed in Malta or Saipan. Moreover, the median spectrum level of the Norway recordings (-134 dBH₀ at 45 Hz) was about 6 dB lower than median levels observed in Saipan and Malta. Although Norway produced the lowest levels of all the recordings sites, non-Gaussian characteristics were nonetheless evident.

E. ELF Noise Model

Examination of APD's from these recordings suggests that the ELF noise from these areas can be modeled as the sum of two processes: (1) a Gaussian background process due to many distant storms, and (2) an impulsive process attributed to a single storm which occasionally dominates the background.⁴ Atmospheric noise was simulated with this model. The impulsive process was generated by filtering a Poisson point process so that the resultant shot process had pulse durations and burst statistics (see Table 1) similar to the measured atmospheric noise. APD's, spectra, and time waveforms of the simulated noise closely resembled those of the measured ELF noise.

With this model one can estimate the performance of nonlinear processing such as hole punching or clipping. For example, with appropriate thresholds, a hole puncher* acts as a linear receiver when only the Gaussian background is present and has no output during the high-level pulses. The effective noise level using a hole puncher can therefore be approximated by

$$N_{\text{eff}} = \frac{N_g}{(1 - k_p)} \quad , \quad (3)$$

where

N_{eff} = effective noise level with hole puncher,

N_g = single-sided spectral level of Gaussian noise process at signal frequency,

k_p = duty factor of pulse process.

For small values of k_p , the performance of the hole puncher is nearly that of an optimum receiver. An optimum receiver's effective noise could be no less than N_g , indicating a hole-puncher degradation of less than $1/(1 - k_p)$ compared to the optimum receiver.

* See Section V for a description of the nonlinearities employed.

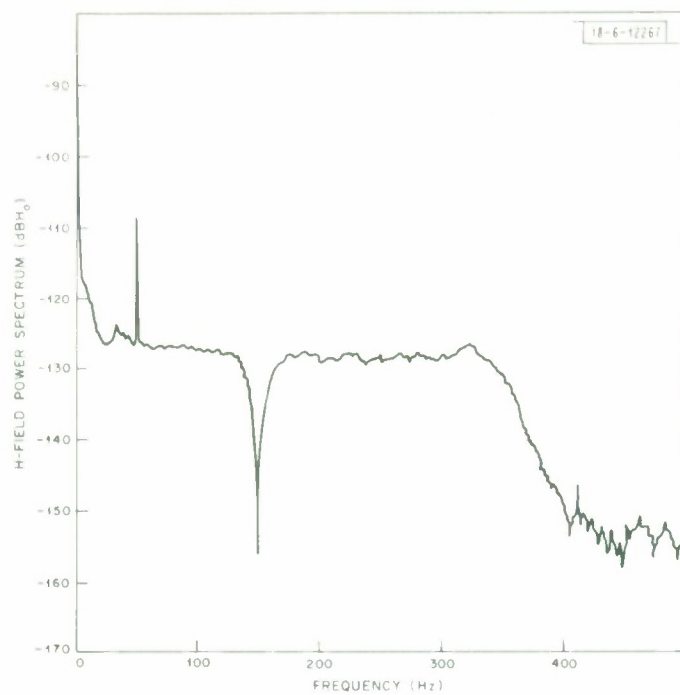


Fig. 11. Spectrum of typical median-level Malta noise.

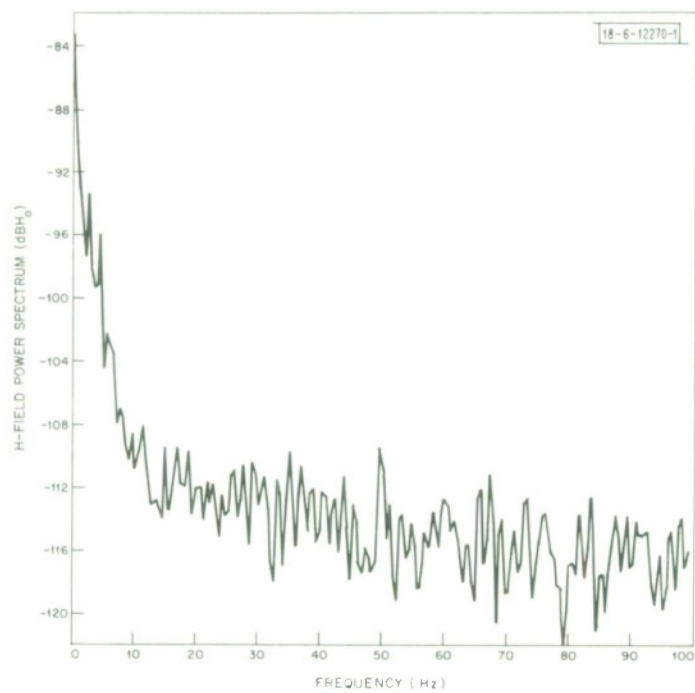


Fig. 12. Spectrum of typical high-level Malta noise.

TABLE I
TYPICAL BURST CHARACTERISTICS OBSERVED
FROM MEASURED H-FIELD DATA

Noise Type	Pulse Rate λ (sec ⁻¹)	Pulse Width T (msec)	$\lambda T = k_p$
High-Level, Saipan	10-13	4-7	0.05-0.07
Median-Level, Saipan	8-10	5-8	0.05-0.07
Median-Level, Saipan	7-8	6-8	0.05-0.06
Median-Level, Malta	10-11	4-5	0.04-0.06
Norway	8-9	3-4	0.02-0.03

Analysis of wideband recordings indicated that k_p was typically less than 0.1 even during local storm activity, indicating a hole-puncher degradation $1/(1 - k_p)$ of less than 1 dB. However, it should be noted that both N_g and k_p are difficult to measure accurately. They depend upon arbitrary definitions of pulses and associated thresholds. Moreover, they depend upon the characteristics of filters used prior to analysis.

F. Antenna Noise

For operation at or near the surface, the dominant source of interference is atmospheric noise. While the attenuation through sea water is small enough to permit communication, at antenna depths of about 100 meters both the signal and atmospheric noise are attenuated enough so that antenna noise becomes a factor. The attenuation in sea water is

$$\alpha_s(f) = 15.3 \sqrt{f \mu_o \sigma_s} \quad , \quad (4)$$

where

f = frequency in Hz,

μ_o = permeability of sea water = $4\pi \times 10^{-7}$ henries/m,

σ_s = conductivity of sea water ≈ 4 mhos/m.

Therefore,

$$\alpha_s(45) \approx 0.23 \text{ dB/m} \quad , \quad (4a)$$

$$\alpha_s(75) \approx 0.30 \text{ dB/m} \quad . \quad (4b)$$

Measurements of sea water conductivity¹³ indicate variations as great as 25 percent in different parts of the world, resulting in more than 10 percent variations in α_s . Furthermore, layers in the ocean can cause changes of α_s as a function of depth.

Electrode pair antennas are currently under development at the Naval Underwater Systems Center, New London Laboratory. Preliminary tests¹⁸ indicate considerable variations in noise spectra with different antenna designs and towing methods. For simulation purposes, Gaussian noise was generated and shaped to match estimated antenna noise spectra.¹⁹

IV. PROCESSING SENSITIVITY TO COMPENSATING FILTER CHARACTERISTICS

To minimize the effects of large spikes, a filter should be used prior to nonlinear processing in order to compensate for the smearing effect of the atmospheric and ocean channels. The compensating filter should operate over a large bandwidth to minimize the duration of the spikes. However, the effects of the compensating filter are complicated by the presence of background atmospheric noise and antenna noise. It is shown in Section IX that a wideband compensating filter can boost high-frequency antenna noise to such a level that it seriously degrades nonlinear processing. It is therefore of great interest to examine the effects of compensating filter bandwidth variations.

Experiments were conducted on several ELF noise recordings in the absence of antenna noise, reducing the upper cutoff frequency of the compensating filter from a maximum of 350 Hz to 80 Hz. The characteristics of the compensating filters were designed to flatten the noise spectrum within the pass band. Both hard limiters and clippers yielded similar results: the upper cutoff frequency could be reduced to 200 Hz with less than 0.5-dB degradation in signal-to-noise ratio; further reduction to 160 Hz and 140 Hz yielded less than 1.0-dB loss, as shown by Table II.

These simulations suggest that the duty factor of the large spikes is small even when the spikes are passed through filters with bandwidths less than 150 Hz. Further examples of this insensitivity were obtained from simulations with Saipan noise which was passed through a simulated ocean layer of 100 meters; the resultant spectrum is illustrated by Fig. 13. Observations from these experiments were:

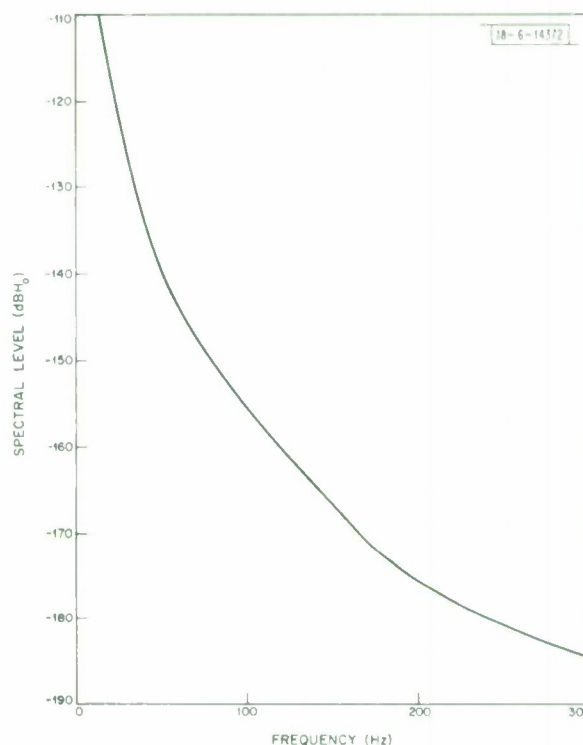
- (a) The low-level noise tapes experienced no significant increase in effective noise due to 100 meters of ocean smearing.
- (b) The high-level noise tapes experienced increases in effective noise of 4 to 6 dB at an antenna depth of 100 meters.

Experiments with different slopes also showed that the processing gains were relatively insensitive to compensating filter characteristics. Best results were obtained by using a filter which flattened or whitened the noise spectrum (and notched dominant power line frequencies), typically boosting high-frequency H-field data at a rate of about 3 dB/octave. However, effective noise levels within 1 dB of these results were obtained with data corresponding to dH/dt (loop antenna outputs). Only a 2-dB degradation compared to the whitening filter was observed using

TABLE II
TYPICAL ELF PROCESSING DEGRADATION (dB)
AS A FUNCTION OF COMPENSATING FILTER UPPER CUTOFF FREQUENCY

Upper Cutoff Frequency (Hz)	Processing Degradation (dB)
350	0
300	0
200	0.0-0.5
160	0.1-0.6
140	0.1-0.8
120	0.2-1.0
100	0.5-1.5
80	1.0-1.8

Fig. 13. Spectrum of high-level Saipan noise at simulated antenna depth of 100 meters.



data proportional to H-field. In summary, experiments did not indicate great sensitivity to compensating characteristics; bandwidths as low as 120 to 150 Hz could be used with less than 1-dB penalty compared to 300- to 350-Hz bandwidths.

V. PROCESSING SENSITIVITY TO NONLINEARITY CHARACTERISTICS

Using the independent sample model as a guideline, a zero memory nonlinearity followed by a matched filter is suggested. The form of the optimal nonlinearity for that model has the following input-output characteristic¹²

$$f(x) = \frac{-d \ln [p(x)]}{dx} \quad (5)$$

where

$f(x)$ = output of nonlinearity,

(x) = input of nonlinearity,

$p(x)$ = probability density function of nonlinearity input.

Substitution of a Gaussian probability density function into Eq. (5) yields a linear function. Whereas analysis of ELF probability density functions indicates that the resultant $f(x)$ has a small linear region for small values of x , large input values (corresponding to prominent lightning strokes) are suppressed. Other more practical nonlinearities which can be specified by a single parameter are hole punchers and clippers which are illustrated by Fig. 14.

In many experiments, a hard limiter (clipper with clip level set near zero) was used as a reference to compare the performance of other nonlinearities. The advantage of a hard limiter is that its performance is independent of receiver gains. Furthermore, since analysis of a hard limiter is relatively straightforward, it has often been used to illustrate various effects of nonlinearities.

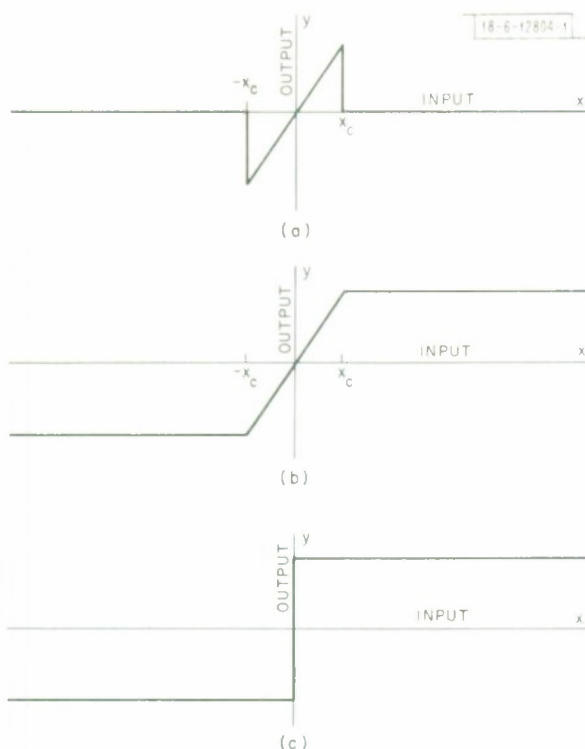


Fig. 14. Nonlinearities used for simulations: (a) hole puncher; (b) clipper; (c) hard limiter.

Experiments with several nonlinearities indicated that

- (a) The performance of "optimal" nonlinearities and hole punchers was very sensitive to gain adjustments.
- (b) Clippers were less sensitive to gain adjustments and yielded nearly as high performance.
- (c) Hard limiters were typically $\frac{1}{2}$ to $1\frac{1}{2}$ dB poorer than clippers, hole punchers, or "optimal" nonlinearities.

Figures 15 and 16 show the observed performance of clippers and hole punchers, using the output signal-to-noise ratio as the performance measure and the hard limiter as the reference.

Figure 15 shows that, with a clipper, typically a 1-dB gain relative to a hard limiter was achieved by setting the clip level, X_c , comparable to the background wideband rms noise level in the absence of large spikes (1 to 4 $\mu\text{amp/m}$).^{*} As the linear region was increased, the gains dropped off and deteriorated rapidly beyond a clip level of 8 $\mu\text{amp/m}$.

Figure 16 shows that the hole puncher did not perform quite as well as the clipper (at least with the experimental values of X_c) with a typical gain of 0.4 dB compared to a hard limiter, and in several cases performed worse than the hard limiter. The cutoff levels which yielded the best gains typically lay between 4 and 8 $\mu\text{amp/m}$, compared to the clipper's best region of 1 to 4 $\mu\text{amp/m}$. At cutoff levels less than 1 $\mu\text{amp/m}$, the performance of the hole puncher deteriorated rapidly since it suppressed most of the input data. In the limit as the cutoff level goes to zero, the input is entirely ignored; as the cutoff level is increased, like the clipper, the hole puncher approaches the performance of a linear receiver.

^{*}Clip levels were measured relative to the input H-field.

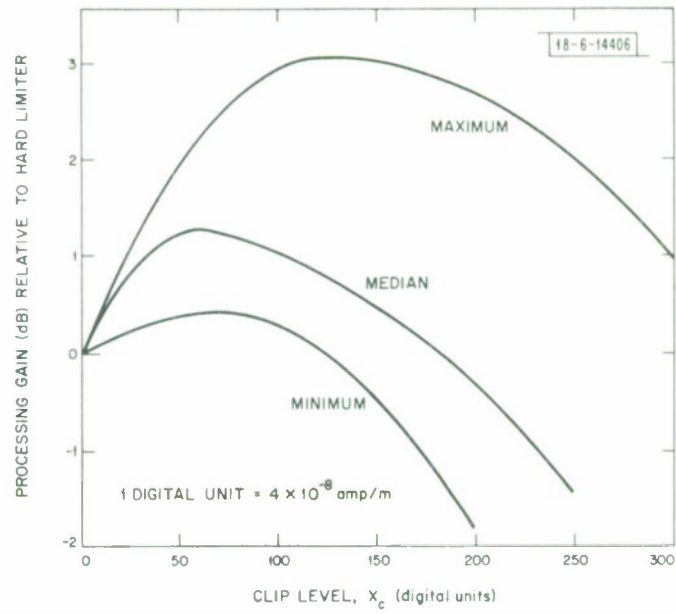


Fig. 15. Clipper gains relative to hard limiter.

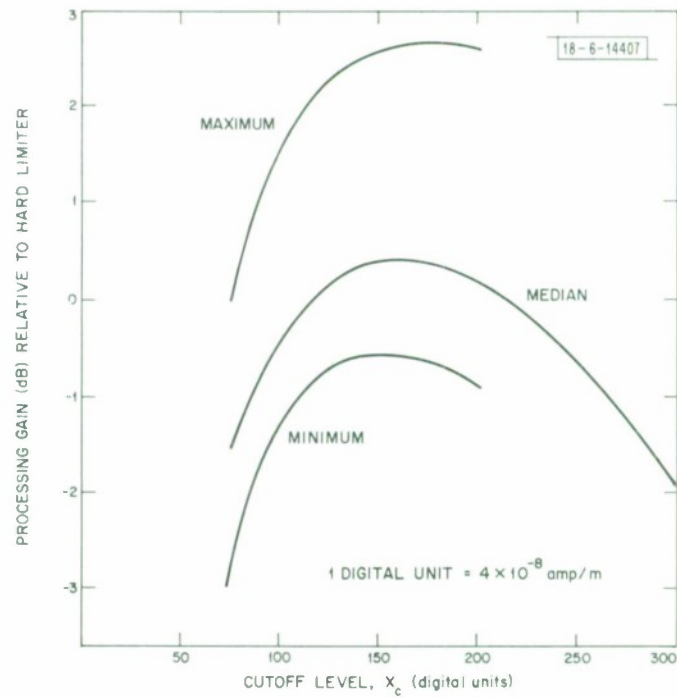


Fig. 16. Hole puncher gains relative to hard limiter.

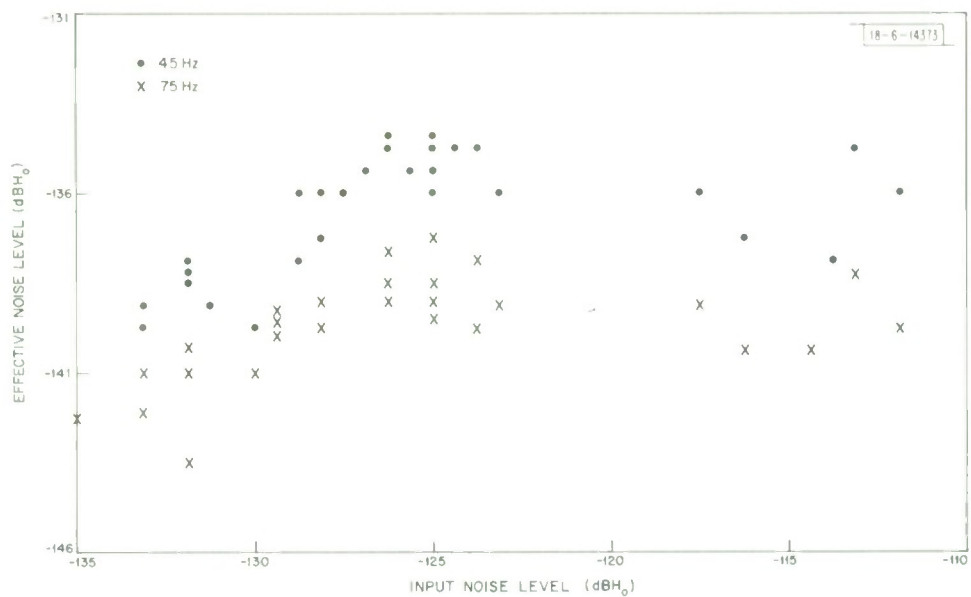


Fig. 17. Effective noise levels vs input noise for Saipan data using clipper.

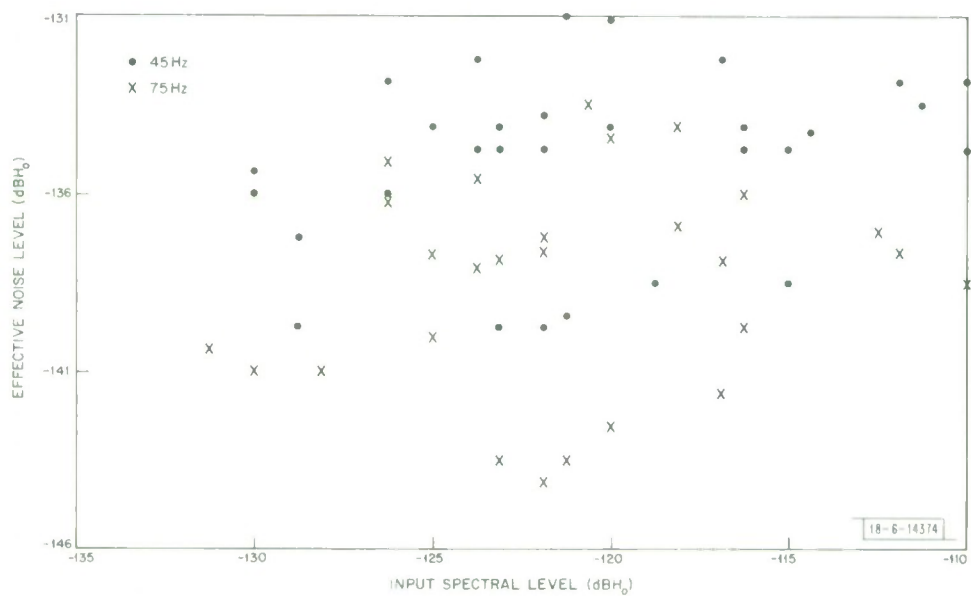


Fig. 18. Effective noise levels vs input noise for Molta data using clipper.

VI. EFFECTIVE NOISE LEVEL SENSITIVITY TO INPUT SPECTRAL LEVELS

Analysis of ELF noise recordings suggests a background process which is relatively constant plus a pulse process which varies considerably with local storm activity and which can cause great variations in spectral levels. Furthermore, since median-level and high-level noise differ primarily in their pulse amplitudes and not significantly in their pulse arrival rate, one might expect nonlinear processing to be relatively insensitive to noise level changes. Simulations using various compensation filters and nonlinearities confirm this expectation.

The insensitivity of effective noise levels to input spectral levels was clearly shown by simulations with Malta and Saipan data. Figures 17 and 18 show effective noise levels vs input noise levels from Saipan and Malta data using a receiver with a clipper. Most of the input noise levels were above median (about -132 dBH_0). For Saipan data the highest effective noise levels were about -134 dBH_0 at 45 Hz and were about -138 dBH_0 at 75 Hz. Similarly, for Malta, the highest observed effective noise levels were about -131 dBH_0 at 45 Hz and -134 dBH_0 at 75 Hz. Fitting straight lines or exponential curves to the Saipan and Malta data yielded slopes of about 0.1 (dB change in effective level/dB change in input level).

Analysis of effective noise level sensitivity to spectral level changes was difficult for Norway recordings because the spectral levels themselves showed so little variation. However, simulations with ten Norway tapes for which the spectral level varied from -132 to -136 dBH_0 at 45 Hz showed no correlation between the higher input levels and the higher output levels. Effective noise levels for these simulations using a clipper (with clip level at $1 \mu\text{amp/m}$) are summarized in Table III. Simulations with a hard limiter showed a similar dispersion but 0.3 to 1.7-dB higher effective noise levels.

TABLE III
EFFECTIVE NOISE LEVELS AND STANDARD DEVIATIONS
FOR TEN NORWAY TAPES (20 SIMULATIONS)

Frequency (Hz)	Median N_{eff} (dBH_0)	Standard Deviation (dB)
40	-139.9	1.7
45	-140.5	1.7
75	-144.3	1.5
80	-145.2	1.5

As it was shown in Section II, these simulation results are insufficient to perform statistical analysis of worst case conditions. To estimate accurately 99 percentile effective noise levels, several thousand simulations could be required. However, because the observed effective noise levels varied so little (including many simulations with high-level input noise), one would not expect significant changes in 99 percentile effective noise levels from the observed values.

VII. PROCESSING SENSITIVITY OF SIGNAL FREQUENCY

Selection of the signal frequency depends upon several considerations including

- (a) Transmitter antenna efficiency,
- (b) Propagation effects,

- (c) Interference to local telephone and power systems,
- (d) Interference from 50- and 60-Hz power radiation,
- (e) Effective noise level variation with frequency.

From these considerations, transmitter frequencies of 40 to 46 Hz or 75 to 80 Hz are of primary interest.

Because propagation losses increase with frequency, ELF background noise attributed to distant storms decreases with frequency. Measurements indicate that the spectral levels decrease above 2 dB/octave for Saipan, 3 to 4 dB/octave for Malta, and about 5 dB/octave for Norway between 40 and 80 Hz.^{16,17} Simulations indicated that effective noise levels are not greatly affected by local storms, indicating that effective noise levels, dominated by background noise, might also decrease with frequency. Experiments confirm this indication. Effective noise levels using hard limiters and clippers at 75 to 80 Hz were consistently 3 to 3½ dB lower than 45-Hz levels for simulations with Saipan and Malta data. Experiments with Norway data indicated a 5- to 6-dB increase in effective noise levels at the higher frequencies.

VIII. PROCESSING SENSITIVITY TO SIGNAL LEVEL

Effective noise levels using nonlinear processing are dependent not only upon input noise characteristics but also upon signal amplitude. In contrast to linear processing, the output signal-to-noise ratio using nonlinear processing is not exactly proportional to the input signal level for a given noise environment. This is illustrated by the theoretical computation of the signal-to-noise ratio at the output of a hard limiter, assuming symmetrically distributed independent noise samples and a constant (DC) signal.

$$\text{SNR} \triangleq \frac{[E(y)]^2}{\text{VAR}(y)} \quad , \quad (6)$$

$$E(y) = P(s + n > 0) - P(s + n < 0) \quad , \quad (7)$$

$$\text{VAR}(y) = E[y - E(y)]^2 = E(y^2) - 2E(y) + E^2(y) \quad , \quad (8)$$

where

$$y = \text{hard limiter output} = \begin{cases} 1 & \text{if } s + n > 1 \\ 0 & \text{if } s + n = 0 \\ -1 & \text{if } s + n < -1 \end{cases} \quad ,$$

$E(\)$ = expected value,

$\text{VAR}(\)$ = variance,

s = signal input,

n = noise input,

$p(s + n)$ = probability density of signal plus noise.

For even functions of $p(n)$,

$$E(y) = 2 \int_0^s p(n) \, dn \quad (9)$$

Therefore, the signal-to-noise ratio at the output of a hard limiter can be expressed as

$$\therefore \text{SNR}_{\text{HL}} = \frac{4 \left[\int_0^S p(n) \, dn \right]^2}{1 - 2 \int_0^S p(n) \, dn + \left[\int_0^S p(n) \, dn \right]^2} \quad , \quad (10)$$

which in general is not proportional to the signal energy, s^2 . However, for very low signal-to-noise ratios, the integral,

$$\int_0^S p(n) \, dn \ll 1 \quad , \quad (11)$$

and can be approximated by

$$s \, p(0) = \int_0^S p(n) \, dn \quad , \quad (12)$$

yielding a signal-to-noise ratio from Eq. (10) of

$$\text{SNR}_{\text{HL}} \doteq 4 s^2 [p(0)]^2 \quad , \quad (13)$$

which is proportional to the signal energy, s^2 .

Experiments using hard limiters and clippers indicated that, for estimated received signal levels and output signal-to-noise ratios of about 0 dB (with 0.1-second integration), a 6-dB variation in signal strength resulted in a signal-to-noise ratio variation of 4.5 to 5.5 dB using Malta data and a signal-to-noise ratio variation of 5.4 to 5.7 dB using Saipan data.

IX. PROCESSING AT DEPTH

It was shown in Section IV that, in the absence of antenna noise, maximum processing gains against noise spikes are obtained by minimizing spike widths with a wideband compensating filter. During operation at depth, this filter should compensate for the low-pass filter effect of the ocean channel which smears the spikes as illustrated by Fig. 19. However, this compensation, which boosts the higher-frequency atmospheric noise, also boosts the higher-frequency antenna noise. At antenna depths of 75 to 100 meters, the ocean compensation can boost the higher-frequency antenna noise so much that it becomes the dominant source of interference. There is thus a trade-off between minimizing the effect of pulses (requiring wide processing bandwidths) and minimizing the effect of antenna noise (requiring narrow processing bandwidths).

Figure 20 shows typical spectra of high-level atmospheric noise at simulated ocean depths* of 100 to 200 meters and estimated spectra of antenna noise for platform speeds of 8, 12, and 14 knots using a 300-meter spaced electrode pair antenna. These spectra illustrate two points. First, at 45 and 75 Hz there are several combinations of antenna speeds and depths where the antenna noise is comparable to the effective noise level, 13 dB below the atmospheric level for this example. Second, at depths greater than 100 meters, the atmospheric noise falls off faster with frequency than does the antenna noise. Consequently, ocean compensation which flattens the atmospheric spectrum overemphasizes the high-frequency antenna noise. This boosting of

* Throughout this section, depth refers to the antenna depth, as apposed to the submarine's depth which might be greater.

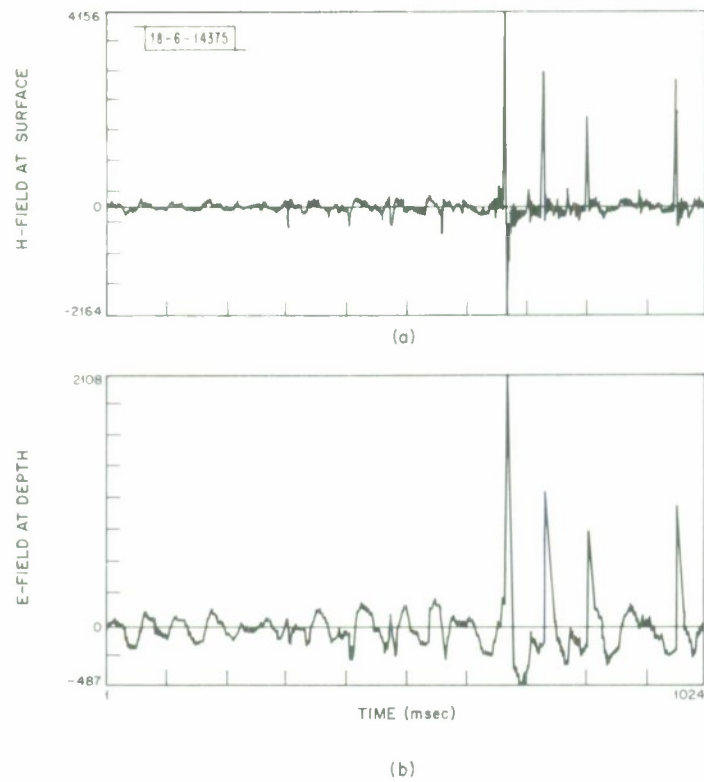


Fig. 19. ELF noise: (a) at the surface; (b) at a simulated depth of 100 meters.

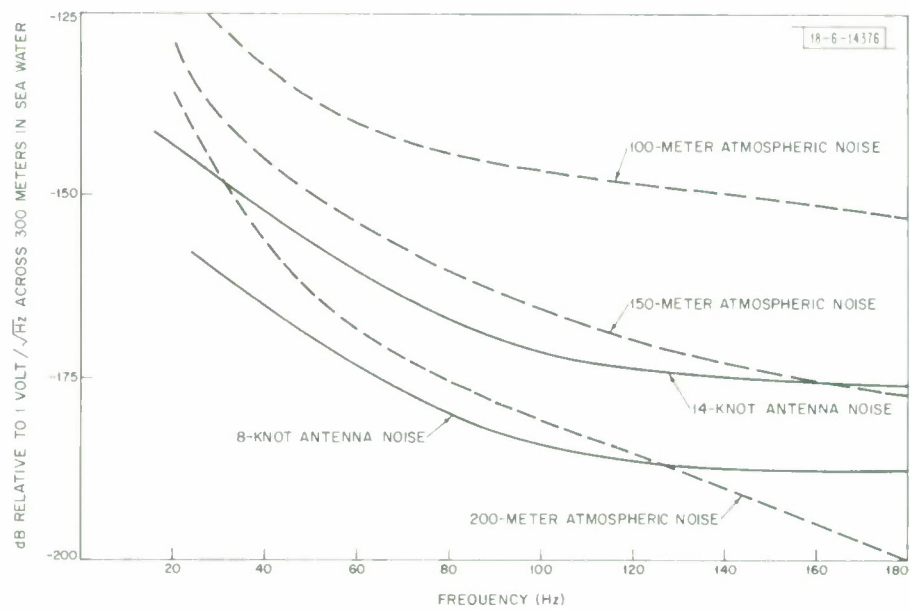


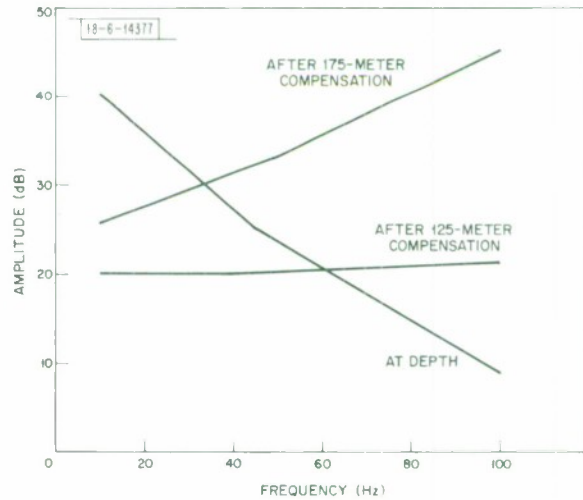
Fig. 20. Spectra of antenna noise and ELF noise at depth.

the high-frequency antennanoise would be irrelevant if linear processing were used. However, with nonlinear processing, the out-of-band noise can spread into the signal band introducing processing degradation.

A. Theoretical Estimate of Antenna Noise Effects

With the ELF noise model of the sum of a Gaussian process and an impulsive process, the effects of added antenna noise can be predicted theoretically. Figure 21 shows that, at antenna depths of 100 to 125 meters, after appropriate filtering the antenna noise and atmospheric noise are fairly flat so that samples from the Gaussian components would be nearly independent. The Gaussian antenna noise level would therefore be added to the background noise level and for small values of k_p (the pulse duty factor) would be added to the effective noise level.

Fig. 21. Spectral shape of simulated E-field antenna noise.



Using a hard limiter, it was shown [Eq. (13)] that the output signal-to-noise ratio with independent samples and small signals depends upon the probability density function, $p(x)$, evaluated at the origin. One can evaluate $p(x)$ at the origin if it is assumed that the antenna noise is an independent Gaussian process with standard deviation σ_A , that the background noise is an independent Gaussian process with standard deviation σ_B , and that the impulsive noise has a duty factor k_p and consistently dominates all other components when the pulses occur. Then

$$p(0) \doteq \frac{1 - k_p}{\sqrt{2\pi} \sqrt{\sigma_B^2 + \sigma_A^2}} \quad , \quad (14)$$

and an effective noise level can be defined as

$$N_{\text{eff}} = \frac{\pi}{2} \frac{\sigma_B^2 + \sigma_A^2}{1 - k_p} \quad . \quad (15)$$

From this expression it can be seen that the effective noise level N_{eff} at depths where the compensated antenna noise spectrum is flat can be approximated by the effective noise level in the absence of antenna noise $\{(\pi/2) [\sigma_B^2/(1 - k_p)]\}$ plus the antenna noise enhanced by $\pi/2$ (about 2 dB), $(\pi/2) \sigma_a^2$.

At greater depths where the high-frequency antenna noise is overcompensated by the filter which whitens the atmospheric noise, foldover effects must be considered. The performance of a nonlinear processor can be seriously degraded by such overemphasis of the high-frequency component even though its energy before processing is far from the signal frequency. For example, hard limiting causes a redistribution of spectral energy which can be computed if the signal is small, if the autocorrelation function of the noise is known, and if the probability density of the input noise is Gaussian. For a continuous process, the signal can be shown to experience a hard limiter loss of 2 dB compared to the total noise power²⁰ and the output spectrum can be obtained from Price's theorem,²¹

$$\rho_o(\tau) = \frac{2}{\pi} \sin^{-1} [\rho_i(\tau)] \quad , \quad (16)$$

which can be expanded:

$$\rho_o(\tau) = .64 \rho_i(\tau) + .11 \rho_i^3(\tau) + .05 \rho_i^5(\tau) + \dots \quad , \quad (17)$$

where

$\rho_o(\tau)$ = normalized autocorrelation function of hard limiter output,

$\rho_i(\tau)$ = normalized autocorrelation function of hard limiter input.

The resultant spectrum is the sum of Fourier transforms of each of the terms above.

$$\Phi_o(f) = K [.64 \Phi_i(f) + .11 \Phi_i(f) * \Phi_i(f) * \Phi_i(f) + \dots] \quad , \quad (18)$$

where

$\Phi_o(f)$ = spectrum of hard limiter output,

$\Phi_i(f)$ = spectrum of hard limiter input,

K = constant, dependent on hard limiter output level,

$*$ denotes convolution.

Spreading of high-frequency energy into the signal band is the result of the input spectrum convolved with itself several times. Similarly, if one considers the high-frequency energy peaked so that the autocorrelation function before limiting is a damped oscillatory function, after limiting, it will have odd harmonics of the original oscillation with greater damping on the higher-order terms. The resultant spectrum will contain peaks at the odd harmonics of the oscillation, and the energy around these peaks will be broadened compared to the original shape due to the narrowing of the higher-order autocorrelation components. In a sample data system where the spectrum is periodic, one might expect degradation due to high-frequency energy (harmonics of peaks in the original spectrum) folding over. For example, with a sample rate of 1000 Hz and a spectral peak at 350 Hz, the third harmonic will result in energy at 50 Hz ($= 350 \times 3 - 1000$).

In summary, at depths of 100 to 124 meters where the antenna noise is approximately flat after the noise compensation filter, the predicted effective noise level using a clipper or hole puncher is approximately the sum of (1) the effective noise level observed in the absence of noise, and (2) the antenna noise level. Similarly, the effective noise using a hard limiter is the sum of (1) the effective noise observed in the absence of antenna noise, and (2) the antenna

noise multiplied by $\pi/2$. At greater depths, an additional loss due to foldover would be expected. Spectral analysis of antenna noise compensated for a depth of 175 meters indicates an additional 1 to 2-dB enhancement of the antenna noise at these depths.

B. Experiments with Simulated Antenna Noise at Depth

Several experiments were conducted with simulated antenna noise to determine foldover effects using various processing bandwidths and nonlinearities. These experiments indicated that (1) relatively narrow processing bandwidths of 100 to 150 Hz are considerably better than wide bands of 300 to 350 Hz at depths greater than 100 meters, (2) foldover effects are negligible at antenna depths less than 100 meters, and (3) experimental results agreed with theoretical predictions.

Simulations with different processing bandwidths were conducted on antenna noise in the absence of atmospheric noise to determine hard limiter degradation compared to linear processing (which is optimum for Gaussian noise). For bandwidths of 90 Hz and compensation for 125 meters, hard limiter results were nominally 1 dB worse than linear processing. For 175-meter compensation and 90-Hz bandwidths, the degradation was about 2 dB. The foldover effect was quite evident for 125-meter compensation and 300-Hz bandwidth where 9- to 10-dB degradations were observed.

To verify theoretical predictions, experiments were conducted using simulated antenna noise and recorded atmospheric noise passed through a simulated ocean filter and subsequently compensated and processed. Experimental results with a processing band of 10 to 100 Hz indicate that, at antenna depths less than 100 meters, about 1 dB or less of processing degradation can be expected for speeds less than 14 knots. As illustrated by Fig. 22, at antenna depths greater than 100 meters, system performance is sensitive to platform speed. From 100 to 200 meters, where atmospheric post-processed noise and antenna noise levels are comparable,

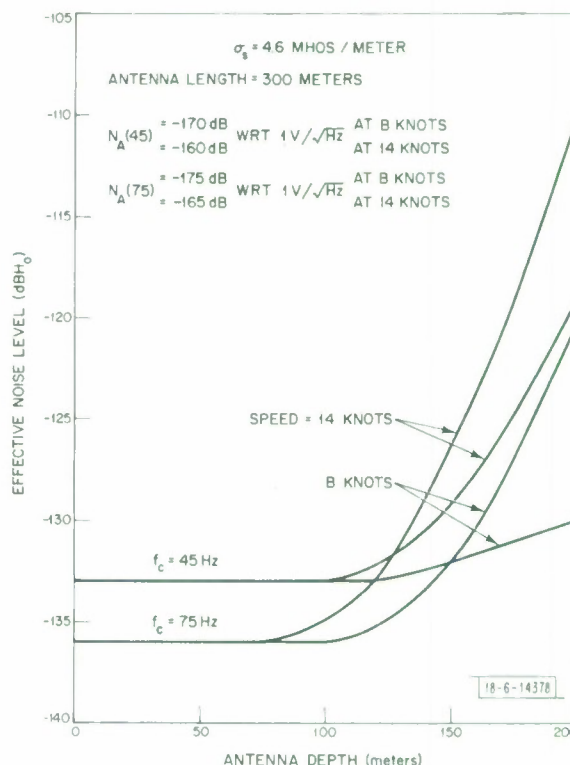


Fig. 22. Typical variation of Soipon effective noise level as a function of antenna depth using clipper.

effective noise levels of clippers with antenna noise can be approximated by adding the post-processed noise level of the atmospheric noise (obtained at the surface) to the antenna noise level measured at the signal frequency. Similarly, experiments with hard limiters supported the theoretical predictions.

X. PROCESSING SENSITIVITY TO INTERFERENCE

In addition to the effects of atmospheric noise and antenna noise, the Sanguine receiver may experience interference from local power systems when operating near shore or from pickup of 60-Hz power generated on the submarine. The amplitude from any of these sources is difficult to predict and has therefore been treated parametrically.

An upper bound for the level of power line interference which can be expected at sea might be the levels observed at the three major recording sites: Saipan, Malta, and Norway. The lowest levels were observed in Saipan where typical values of -130 dBH^* at 60 Hz were observed. In Europe, the interference, which is at 50 Hz, might be considerably higher. Observed levels at the Malta site ranged from -105 to -125 dBH depending upon time of day, season, and antenna orientation. Similarly, levels observed in Tromsø, Norway ranged from -100 to -120 dBH . It would be desirable to extrapolate these levels to those expected several miles at sea. However, such analysis would require detailed information about the balance of the power lines and their geographical distribution to estimate their near field distribution. Similarly, there exist insufficient data to estimate 60-Hz interference radiated from submarine equipment.

The performance of a hole puncher or clipper in the presence of interference can be predicted theoretically if the noise samples are independent, if the background noise and interference are significantly below the clip level, and if the duty factor of the pulse process is small. The hole puncher or clipper can then be characterized as linear in the absence of pulses and as a hard limiter or blanker when pulses are present. Since the MSK signals have a pseudo-random bit stream modulation, the interference at the matched filter output resembles noise, the variance of which can be approximated from the signal and interference spectra†

$$N_1 = K \int_{-\infty}^{\infty} \Phi_I(f) \cdot \Phi_S(f) df \quad , \quad (19)$$

where

$K = \text{constant},$

$\Phi_I(f) = \text{interference spectrum},$

$\Phi_S(f) = \text{MSK signal spectrum}.$

The spectra of MSK signals depend upon the center frequency, deviation frequency, chip duration, and the carrier phase at the chip boundaries.⁶ The mathematical expression for the spectra used in simulations (with peak phase switching) is

* dBH is defined in this report as dB wrt 1 omp/m.

† The spectral computation is valid only if the interference experiences random phase shifts compared to the MSK signals. At certain frequencies and phases, the interference can have a 3-dB greater effect than the spectral computation indicates. Furthermore, due to the finite integration times, the corresponding spectra of the interference are slightly smeared.

$$\Phi_S(f) = \left[\left(\frac{\sin 2\pi fT}{2\pi\sqrt{T}} \right) \left(\frac{f_2^2 - f_1^2}{f^2 - f_1^2} \right) \left(\frac{f}{f^2 - f_2^2} \right) \right]^2, \quad (20)$$

where

f = frequency in Hz,

f_1 = center frequency - deviation frequency (Hz),

f_2 = center frequency + deviation frequency (Hz),

T = chip duration (seconds).

For simulation purposes, it was convenient to use chip durations which were integral multiples of the sampling interval (1 msec), thereby constraining the MSK parameters. Typical parameters were carrier frequencies of 43.65 and 75.40 Hz, frequency deviation of 3.967 Hz, and a chip duration of 63 msec. As illustrated by Fig. 23, power line frequencies are attenuated by more than 30 dB* except for the combination of 50-Hz power lines and 43.65-Hz signaling frequency.

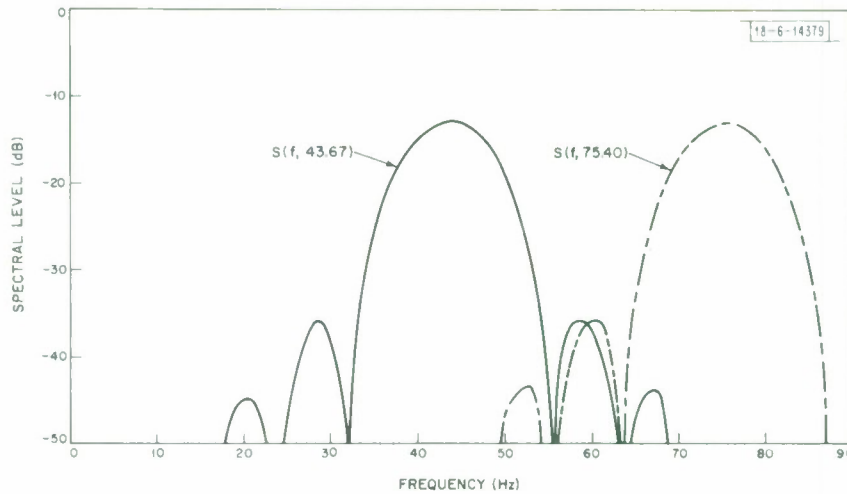


Fig. 23. Normalized MSK spectra with carrier frequencies of 43.65 and 75.40 Hz used for simulations.

As the interference level increases so that the clip level is exceeded in the absence of pulses, two effects are observed: (1) the signal and interference spectra become distorted — harmonics of each and cross product terms are generated, and (2) the signal is suppressed. Similar distortion and signal suppression are experienced with a hard limiter. Figures 24 and 25 illustrate the effects of 50- and 60-Hz interference on MSK signals centered at 43.65 and 75.40 Hz with hard limiting and clipping receivers. Shown as a reference is the predicted interference effect on a linear receiver operating with a noise background equal to the effective noise level. These figures illustrate several points:

- (1) High levels of interference not only add noise, but also suppress the signal using either the hard limiter or clipper.

* That is, if there were equal power MSK signal and sine wave interference at the matched filter input and no noise, the output signal-to-noise ratio or signal-to-interference ratio (average over all phases of the sine wave interference) would be greater than 30 dB.

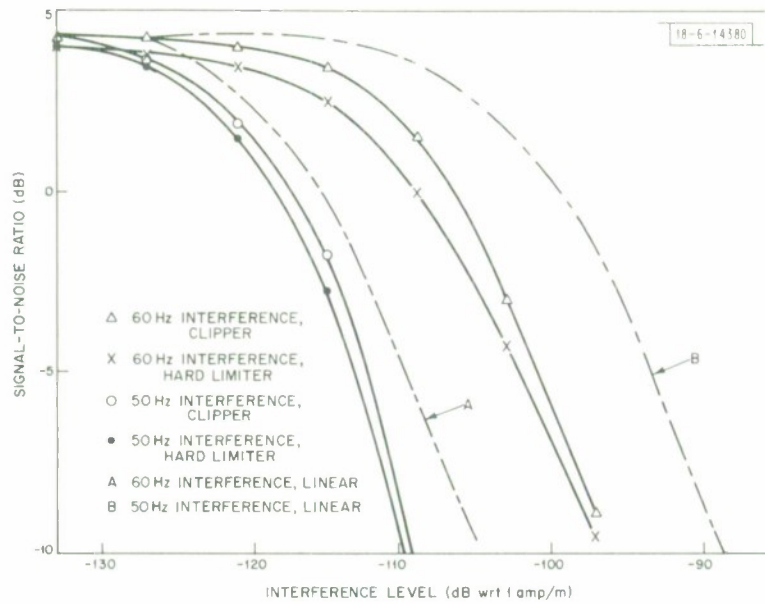


Fig. 24. Interference effects using MSK signals.

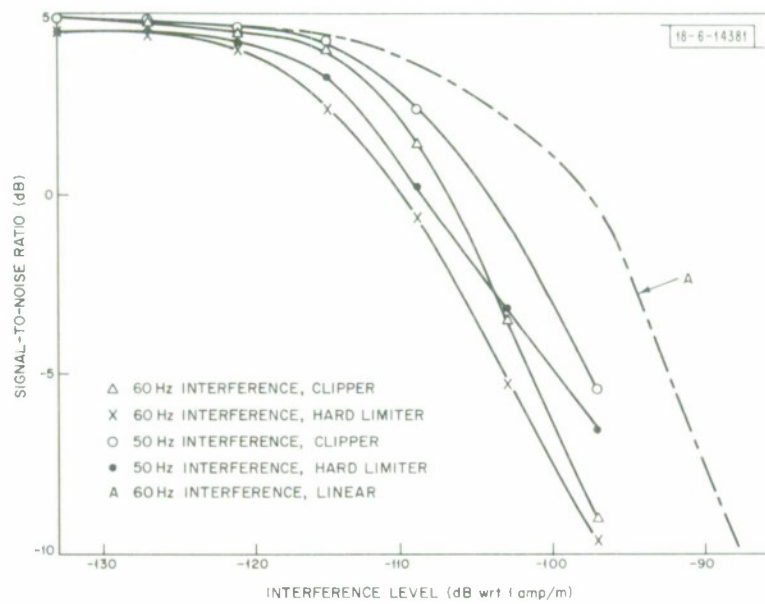


Fig. 25. Interference effects using MSK signals.

- (2) Clipper performance closely follows that of the hard limiter, offering a maximum improvement of 1 to 2 dB in the intermediate range where less than 5 dB of interference degradation is experienced.
- (3) Operation in the 43-Hz range is considerably more susceptible to power line interference, particularly at 50 Hz, than is the higher-frequency signal.

Simulations with high-level Saipan noise with a carrier frequency of 75.4 Hz indicated that the signal-to-noise ratio was degraded by less than $\frac{1}{2}$ dB for 60-Hz interference levels up to approximately -120 dBH.*

For greater levels of interference, 60-Hz interference degraded the signal-to-noise ratio by about 1 dB more than equal levels of 50-Hz interference. This suggests that, for these values of interference, 60-Hz interference effects might be reduced by about 1 dB if the MSK spectra were modified to have a lower spectrum level at 60 Hz. For simulation purposes, a chip duration of 0.063 second was convenient; however, a small change in the chip duration T can shift the spectrum nulls to coincide with 60 Hz, as shown by the sine term of Eq. (20).

TABLE IV
MSK PARAMETERS AND NORMALIZED SPECTRAL LEVELS
AT POWER LINE FREQUENCIES

T (msec)	f_c (Hz)	$(f_2 - f_1)/2$ (Hz)	$\Phi_S(50)$ (dB)	$\Phi_S(60)$ (dB)
63	43.65	3.97	-19	-36
63	75.40	3.97	-47	-36
67	70.90	3.73	-44	-48
67	41.05	3.73	-28	-59
58	81.90	4.31	-53	-59
58	47.41	4.31	-14	-49
63	83.33	3.97	-52	-43

Table IV shows several MSK parameters compatible with a 1000-Hz sampling rate and their normalized spectral levels at 50 and 60 Hz. The MSK signal parameters with the lowest spectral values at 50 and 60 Hz are a chip duration of 58 msec, a center frequency of 81.9 Hz, and a frequency deviation of 4.31 Hz.

A. Notch Filtering

Notch filters can be used to reduce prominent power line interference. However, a notch filter has a ringing impulse response which decays at a rate proportional to its notching bandwidth. Although the energy associated with this ringing is quite low for narrow notches, individual lightning spikes are often so great that their ringing can be seen above the background for many filter time constants. Notch filters might therefore be expected to degrade system performance in the absence of prominent power lines. To reduce the ringing of the large spikes, a clipper can be used preceding the notch filter but following the compensation filter.

* Simulations with various signal levels yielded similar results.

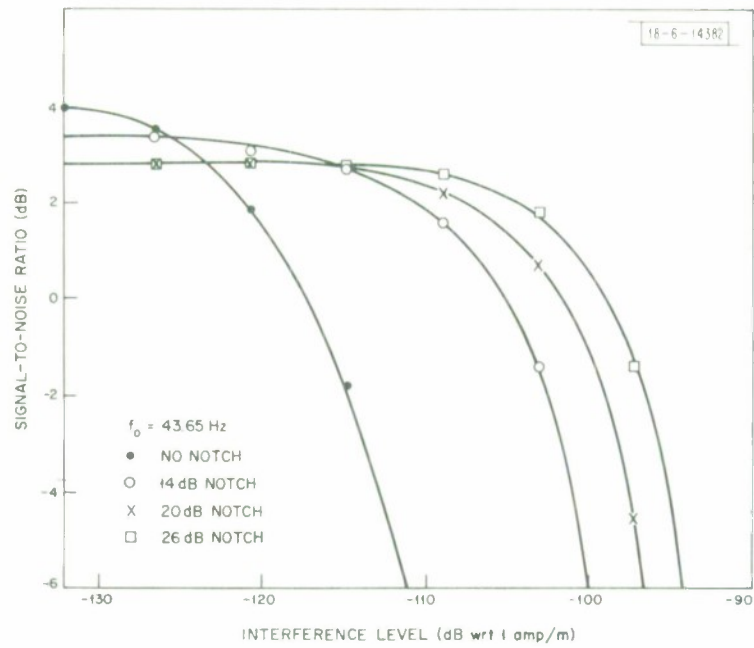


Fig. 26. Interference effects of 50 Hz using notch filters.

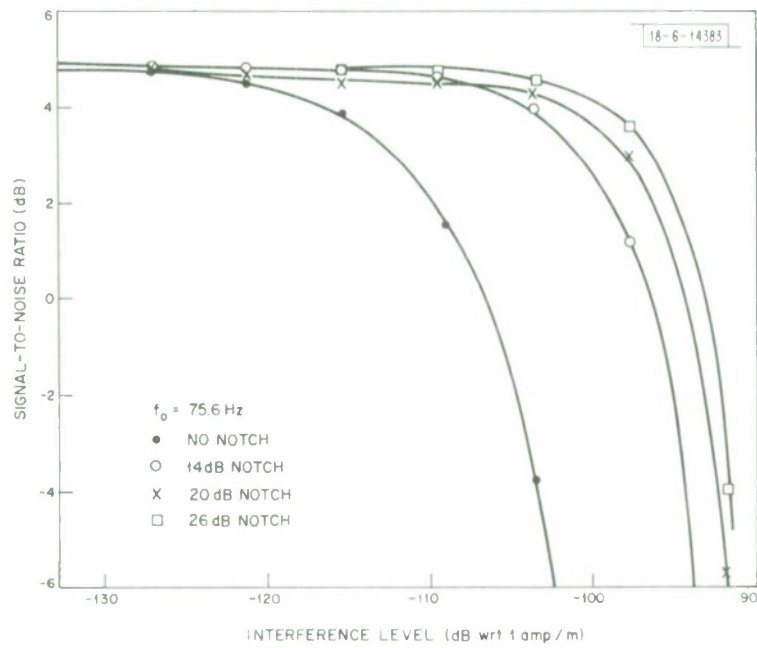


Fig. 27. Interference effects of 60 Hz using notch filters.

An alternative to notch filtering is an estimator subtractor. Since the power line interference can be expected to be relatively constant in amplitude and frequency over a period of several minutes, it can be estimated by using a linear matched filter (or a matched filter preceded by a clipper) and subsequently subtracted. Analogous to the ringing effect of large spikes on notch filters, the estimator's output is influenced by large spikes. Because of the relative simplicity of notch filters, they have been used for simulation experiments.

Experiments have been conducted with a recursive notch filter, with a pair of complex conjugate poles and a pair of complex conjugate zeros, defined by the following difference equation:

$$Y(n) = X(n) - 2R_Z \cos(K_S f_Z) X(n-1) + R_Z^2 X(n-2) \\ + 2R_P \cos(K_S f_P) Y(n-1) - R_P^2 Y(n-2) \quad , \quad (21)$$

where

$Y(i) = i^{\text{th}}$ output sample,

$X(i) = i^{\text{th}}$ input sample,

R_Z = distance from zero to origin in Z-plane,

R_P = distance from pole to origin in Z-plane,

f_Z = zero frequency,

f_P = pole frequency,

$K_S = 2\pi/\text{sample rate}.$

The depth of the notch is closely approximated by²²

$$D_N = -20 \log_{10} \left(\frac{1 - R_Z}{1 - R_P} \right) \quad , \quad (22)$$

when $f_Z = f_P$. Narrow notches can be obtained by placing the poles and zeros near the unit circle on the Z-plane ($R_Z \doteq R_P \doteq 1$).

Simulations indicate that, if a clipper is not used prior to the notch filter, a noticeable degradation compared to no notch filter is experienced in the absence of dominant power line interference. These degradations are a function of the input noise characteristics; values of 1 to 2 dB were observed with high-level Saipan data. With a clipper set slightly above the background noise level, notches of 14, 20, and 26 dB with parameters shown by Table V produced less than $\frac{1}{2}$ -dB degradation in the absence of power line interference when followed by either a hard limiter or clipper.* With a signal frequency of 75.4 Hz and a notch at 60 Hz (including a clipper), no measurable degradation due to the notch filter was observed. Simulation results at various interference levels with various notches are shown in Figs. 26 and 27. At a signal frequency of

* The setting of the clip level preceding the notch filter was not critical at either signal frequency. At low levels of interference, notch filter clip levels set about at the background level produced slightly (0.1 to 0.3 dB) better signal-to-noise ratios than higher clip levels. However, as the interference level approached the clip level, a noticeable degradation of about 1 dB was experienced.

TABLE V
TYPICAL PARAMETERS USED
IN NOTCH FILTER EXPERIMENTS

R_p	R_z	D_N (dB)
0.99	0.998	14
0.98	0.998	20
0.98	0.999	26

75.4 Hz and interference frequency of 60 Hz, use of a 26-dB notch filter (preceded by a clipper) showed no noticeable signal-to-noise ratio degradation for power line levels up to -104 dBH.* Greater levels degraded performance rapidly. Similarly, with a signal frequency of 43.65 Hz and interference at 50 Hz, a 26-dB notch allowed high levels of interference (up to -110 dBH) without noticeable degradation. However, as illustrated by Fig. 27, the notch filters degraded system performance by as much as 1 dB in the absence of power line interference (probably due to signal distortion through the notch filter).

XI. CONCLUSIONS

Based upon simulation experiments described in this report, the recommended noise processor uses a clipper to suppress the effect of large spikes. The recommended configuration (shown by Fig. 28) for the Sanguine receiver consists of an inverse ocean filter, a compensation

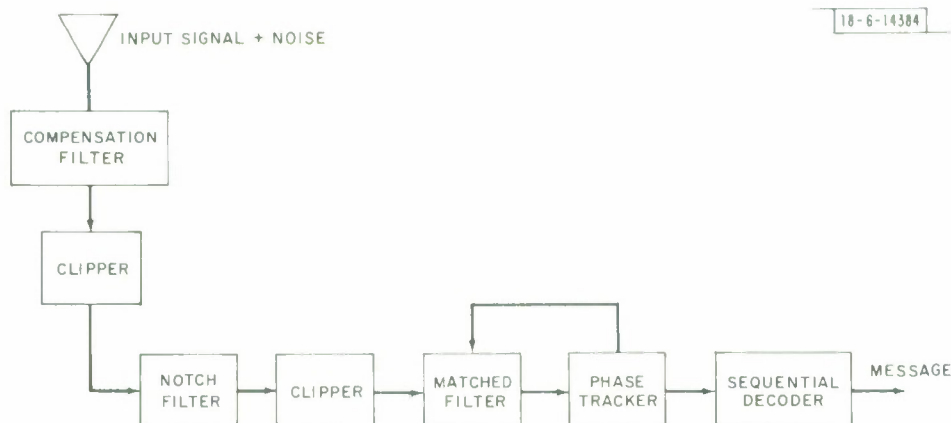


Fig. 28. Recommended Sanguine receiver configuration.

or whitening filter, a notch filter (with an input clipper set above the background noise level and expected power line interference level), a second clipper (set approximately at the background noise level), a matched filter, phase tracker, and decoder. This receiver has been implemented on a small digital computer.³ Its performance in terms of required signal power or effective noise level is 15 to 20 dB better than that of a linear receiver and is not critically sensitive to parameter values such as clip levels or filter characteristics. Analysis of an ELF noise model⁴

* It should be noted that the poles and zeros were matched very closely with the simulated power line interference. If deeper notches were used, more complex filters would be required to maintain stability and to widen the notch sufficiently to guarantee that the power line frequency was adequately suppressed.

indicates that the performance of the recommended receiver is within 1 dB* of the theoretically optimum structure⁵ which is considerably more complex.

Because of the limitation on available noise recordings and processing time, the simulations described in this report cannot precisely cite the 99 percentile effective noise for any of the locations of interest. Moreover, fluctuations in recording calibrations of 1 to 2 dB limit the accuracy with which absolute values of effective noise may be measured.

At this stage of development, measurements are being conducted to estimate more accurately effective noise levels. Continuing antenna development and associated measurements at sea will also yield better estimates of antenna noise characteristics and power frequency interference levels. Further simulations will undoubtedly cause refinement of receiver parameter values. The basic configuration, however, is not expected to be significantly altered.

TABLE VI
ESTIMATED EFFECTIVE NOISE LEVELS

	Signal Frequency (Hz)	Median (dBH _o)	Standard Deviation (dB)	Worst Case (dBH _o)
Saipan	45	-137	1.6	-134
	75	-141	1.4	-138
Malta	45	-136	2.4	-131
	75	-139	3.0	-134
Norway	45	-140	1.7	-137
	75	-144	1.5	-141

The values in Table VI represent observed median and worst case effective noise levels using the recommended receiver at depths and speeds where antenna noise is insignificant. The relatively small standard deviation of effective noise levels compared to input spectral levels reduces the uncertainty in predicting worst case receiver performance compared to wide fluctuations in input spectral levels.

The effective noise levels, together with data rates and required decoder signal-to-noise ratios, determine the required signal energy needed at the receiver. The required transmitter power as a function of signal frequency can then be determined from minimum received signal energy and analysis of propagation effects.

In designing the Sanguine system, performance sensitivity to several parameters is of great interest. The major results described in the preceding sections can be summarized as follows.

- (1) Sensitivity to compensating filter: processing bandwidth reductions from 330 to 100 Hz increased effective noise levels by less than 1 dB.
- (2) Sensitivity to nonlinearity: (a) clippers yielded 0.5 to 1.5 dB better signal-to-noise ratios than hard limiters; (b) hole punchers performed nearly as well as clippers but were more sensitive to level settings.
- (3) Sensitivity to signal level: effective noise levels ($2H_s^2 T_s / \text{SNR}$) were nearly independent of received signal strength at the expected maximum range. A 6-dB change in signal would cause a 5- to 6-dB change in signal-to-noise ratio.

* Derived from approximate analysis of limited data.

- (4) Sensitivity to signal frequency: the effective noise levels at 75 Hz were 3 to 4 dB lower than at 45 Hz.
- (5) Sensitivity to input level: a 10-dB change in input noise level typically resulted in a 1-dB change in effective noise level.
- (6) Effects of antenna noise: at antenna depths up to 175 to 200 meters, the effects of the antenna noise can be approximated by adding it to the effective noise level.
- (7) Effects of power line interference: power line levels up to -104 dBH at 60 Hz with a signal frequency of 75 Hz, and levels up to -110 dBH at 50 Hz with a signal frequency of 44 Hz, can be notch filtered with less than 0.5-dB degradation in signal-to-noise ratio.

APPENDIX A

TWO-SENSOR PROCESSING OF ELF NOISE

This report has described ELF noise processing using a single antenna, namely, an electrode pair antenna, trailed behind the submarine. Such an antenna has a figure 8 beam pattern. Signal reception is therefore severely limited when the submarine is moving nearly perpendicularly to the propagation path.

The development of an antenna whose beam pattern is orthogonal* to the electrode pair would obviate this problem; the antenna outputs after appropriate filtering† could be added to provide omnidirectional coverage. Alternatively, the outputs could be weighted to steer an effective beam toward the received signal, an approach optimum for Gaussian isotropic noise. For ELF noise, which is neither isotropic nor Gaussian, a more sophisticated procedure is suggested. This appendix summarizes an analysis by J. E. Evans.²³

Using an ELF noise model consisting of a Gaussian background plus a pulse process, Evans has described an "optimum" receiver using two sensors, estimated its performance compared to hole punchers and clippers using only one sensor, and suggested simplified receiver configurations. He shows that the optimum receiver combines the antenna outputs to form two beams — one directed toward the received signal, and one orthogonal to the received signal. The data from both beams are used to estimate the pulses on the signal beam for subsequent correlation.

The performance of the two-sensor processor is generally dependent on the relative angle of arrival of the signal and the dominant pulse interference. If the pulses arrive from the same direction as (or 180° from) the signal, clearly the second sensor serves no useful function. If the pulses arrive from a direction orthogonal to signal, they do not have to be subtracted, since the null in the beam pattern suppresses them. Furthermore, the pulses must arrive from a relatively narrow angular sector, since their angle of arrival must be estimated before their component in the signal direction can be subtracted.

Examination of the angular distribution of pulses in Norway and Malta indicated that the direction of arrival of larger spikes was spread over a greater angular sector than might be expected from examining thunderstorm maps. Furthermore, computation of pulse to background noise ratios indicated that estimation receivers would not perform measurably better than nonlinear processing previously described.

A more promising use of the two sensors is utilizing the correlation between the background noise processes from the orthogonal antennas. The receiver would (1) form two orthogonal channels or beams, one pointed toward the transmitter, (2) process each channel using nonlinear processing, and (3) subtract an estimate of the correlated noise of the orthogonal channel from the signal plus noise of the signal channel. The appropriate receiver output is given by

$$r(t) = s(t) + n_s(t) - \rho n_o(t) \quad , \quad (A-1)$$

* A trailed loop antenna is under development at Lincoln Laboratory, although its noise characteristics presently preclude its feasibility. Actually, orthogonality is not required as long as the beams are oriented differently.

† The frequency characteristics of a loop antenna (sensitive to dH/dt) and the electrode pair antenna (sensitive to E -field) differ, requiring different filters.

where

$s(t)$ = signal component after nonlinear processing and matched filtering,

$n_s(t)$ = noise component on signal channel after nonlinear processing and matched filtering,

$n_o(t)$ = noise component on orthogonal channel after nonlinear processing and matched filtering,

ρ = normalized correlation coefficient between channels after nonlinear processing, before matched filtering.

It can be shown that ρ must be averaged over many matched filter integration periods, the maximum of which is dependent upon the stationarity of the correlation on the two channels. The reduction in effective noise level in dB is $10 \log_{10}(1 - \rho^2)$. It should be noted that the reduction is small if the noise is (1) nearly isotropic, (2) predominantly on the signal channel, or (3) predominantly on the orthogonal channel.

Theoretically, it is difficult to predict the maximum attainable ρ from available data, since it is a function of the nonlinear processor characteristics as well as noise statistics. Limited experimental results indicated 0.7- to 3-dB improvements compared to single-sensor processing. These estimates did not include possible further gains using temporal correlation.

APPENDIX B

PROCESSING SENSITIVITY TO SAMPLE RATE

The sampling rate used for the simulations discussed in this report was 1000 Hz. This value was chosen to be the same as digital recordings of the wideband field measurements which employed a band of about 10 to 350 Hz. Experiments indicated that smaller bandwidths (with upper cutoff frequencies of 100 to 150 Hz) would yield little degradation when operating at shallow depths and would significantly reduce foldover effects when operating at depth of 100 meters or more when antenna noise is a major consideration. The reduced bandwidth suggests that a lower sampling rate might be used to relax the speed requirements for a real-time digital receiver.

Reduction of the sampling rate might affect two areas:

- (1) The design and performance of receiver filters, particularly the inverse ocean.
- (2) Nonlinear foldover effects, particularly with antenna noise at depth. To estimate the foldover effect, preliminary tests have been made with a reduced sampling rate introduced after the receiver filters, preceding the nonlinearity. Simulations were conducted with signal frequencies of about 44 and 75 Hz, using clippers and hard limiters and simulated depths of 125 and 175 meters. A processing band of about 100 Hz was used.

From Fig. B-1, one can see the upward slope of the energy in the pass band due to the antenna noise. As the sample rate is reduced, the spectral energy is redistributed about the sample frequency as illustrated by Fig. B-2. With nonlinear processing, foldover or aliasing is a potential problem. Figure B-3 illustrates the spectral smearing effect of a clipper. When the sample rate is reduced, the out-of-band energy, introduced by clipping, can fold into the signal band.

Compared to 1000-Hz sampling, a 500-Hz sampling rate introduced degradations of less than 0.4 dB using a clipper and less than 0.6 dB using a hard limiter. Further sample rate reduction to 250 Hz introduced losses of less than 1 dB using a clipper and less than 2 dB using a hard limiter. In addition to their better performance at reduced sample rates, the clipper provided from 0.2 to 1.0 dB more gain than the hard limiter using a sampling rate of 1000 Hz.

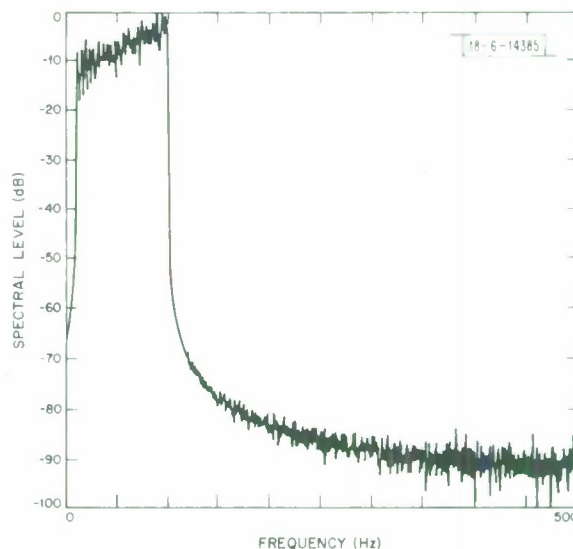


Fig. B-1. Spectrum of ELF noise whitened from depth of 125 meters plus antenna noise in 100-Hz bandwidth, with 1000-Hz sampling rate.

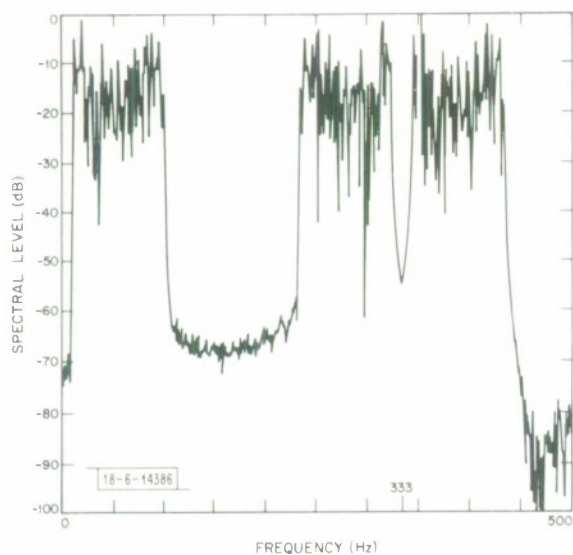


Fig. B-2. Spectrum of ELF noise whitened from depth plus antenna noise in 100-Hz bandwidth, with 333-Hz sampling rate.

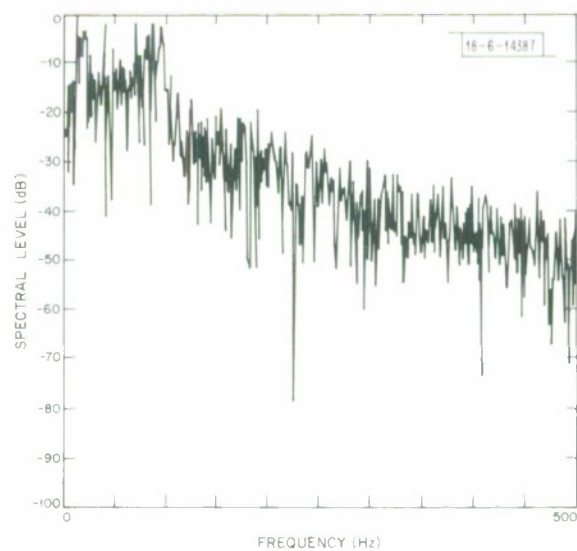


Fig. B-3. Spectrum of ELF noise whitened after clipping using 1000-Hz sampling rate.

REFERENCES

1. S. L. Bernstein, "A Sanguine Receiver Structure," Technical Report 488, Lincoln Laboratory, M. I. T. (limited distribution).
2. D. A. McNeill, "A Simulation Facility for Communication Systems," Technical Report 489, Lincoln Laboratory, M. I. T. (27 December 1971).
3. S. L. Bernstein, A. S. Griffiths, D. A. McNeill and I. Richer, "An Experimental Sanguine Receiver," Technical Report 492, Lincoln Laboratory, M. I. T. (limited distribution).
4. J. W. Modestino, "A Model for ELF Noise," Technical Report 493, Lincoln Laboratory, M. I. T. (16 December 1971).
5. J. W. Modestino, "A Theoretical Optimum ELF Receiver Structure," Technical Report 494, Lincoln Laboratory, M. I. T.
6. B. E. White, "A Derivation of the Spectra of N-ary Orthogonal Continuous-Phase FSK Waveforms for ELF/VLF Communications," IEEE Trans. Commun. Tech. COM-19, 536 (1971).
7. J. E. Evans, "Preliminary Analysis of ELF Noise," Technical Note 1969-18, Lincoln Laboratory, M. I. T. (26 March 1969), DDC AD-691814.
8. F. Horner, "Radio Noise from Thunderstorms," Advances in Radio Research, Vol. II (Academic, New York, 1964).
9. D. P. White and D. K. Willim, "ELF Propagation Study (Phase I - Summer 1970)," Technical Note 1971-3, Lincoln Laboratory, M. I. T. (11 January 1971), DDC AD-718100.
10. J. M. Wozencraft and I. M. Jacobs, Principles of Communication Engineering (Wiley, New York, 1965).
11. R. Lerner and V. Algazi, private communications.
12. O. Y. Antonov, "Optimum Detection of Signals in Non-Gaussian Noise," Radio Eng. and Elect. Physics 12, 541 (1967).
13. "Sanguine System Design Study," NAVELEX Document (December 1970), not generally available.
14. I. Richer, private communications.
15. E. T. Pierce, "The Thunderstorm as a Source of Atmospheric Noise at Frequencies Between 1 and 100 KHz," SRI, DASA 2299, Contract DASA-1-68-C-0073 (June 1969).
16. "Final Atmospheric Noise Report," Westinghouse, TR 69-8 HL, Contract 0039-69-C-1541 (March 1969).
17. "Atmospheric Noise Measurements at Malta and Guam for the Summer Season 1969," Radio Corporation of America, Spec. Topic Memo 29, Contract 0039-68-C-1518.
18. L. Herrold and D. O'Brian, "Empirical Study of Buoyant Electrode Pair Antennas," NUSL Report NL-3032 (1971).
19. D. O'Brian, NUSL, private communications.
20. S. L. Bernstein, private communications.
21. R. Price, "A Useful Theorem for Non-Linear Devices Having Gaussian Inputs," Trans. IRE, PGIT 1T-4, 69 (1958).
22. B. Gold and C. M. Rader, Digital Processing of Signals (McGraw-Hill, New York, 1969).
23. J. E. Evans, private communications.

DISTRIBUTION

Chief of Naval Operations
Attn: Capt. R. Wunderlich (OP-941P)
Department of the Navy
Washington, D. C. 20350

Chief of Naval Research (Code 418)
Attn: Dr. T. P. Quinn
800 North Quincy Street
Arlington, Virginia 22217

Computer Sciences Corporation
Systems Division
Attn: D. Blumberg
6565 Arlington Boulevard
Falls Church, Virginia 22046
(3 copies)

IIT Research Institute
Attn: Dr. D. A. Miller, Div E
10 West 35th Street
Chicago, Illinois 60616

Institute for Defense Analyses
Attn: Mr. N. Christofilos
400 Army-Navy Drive
Arlington, Virginia 22202

Naval Civil Engineering Laboratory
Attn: Mr. J. R. Allgood
Port Hueneme, California 93043

Naval Electronics Laboratory Center
Attn: Mr. R. O. Eastman
San Diego, California 92152

Naval Electronic Systems Command
Attn: Capt. F. L. Brand, PME 117
Department of the Navy
Washington, D. C. 20360

Naval Electronic Systems Command
Attn: Mr. J. E. Don Carlos, PME 117T
Department of the Navy
Washington, D. C. 20360
(2 copies)

Naval Electronic Systems Command
Attn: Cdr W. K. Hartell, PME 117-21
Department of the Navy
Washington, D. C. 20360
(10 copies)

Naval Electronic Systems Command
Attn: Dr. B. Kruger, PME 117-21A
Department of the Navy
Washington, D. C. 20360

Naval Electronic Systems Command
Attn: Capt. J. V. Peters, PME 117-21
Department of the Navy
Washington, D. C. 20360
(2 copies)

Naval Electronic Systems Command
Attn: Mr. E. Weinberger, PME 117-23
Department of the Navy
Washington, D. C. 20360
(2 copies)

Naval Facilities Engineering Command
Attn: Mr. G. Hall (Code 054B)
Washington, D. C. 20390

New London Laboratory
Naval Underwater Systems Center
Attn: Mr. J. Merrill
New London, Connecticut 06320
(4 copies)

The Defense Documentation Center
Attn: DDC-TCA
Cameron Station, Building 5
Alexandria, Virginia 22314

DOCUMENT CONTROL DATA - R&D		
(Security classification of title, body of abstract and indexing annotation must be entered when the overall report is classified)		
1. ORIGINATING ACTIVITY (Corporate author) Lincoln Laboratory, M. I. T.		2a. REPORT SECURITY CLASSIFICATION Unclassified
		2b. GROUP None
3. REPORT TITLE ELF Noise Processing		
4. DESCRIPTIVE NOTES (Type of report and inclusive dates) Technical Report		
5. AUTHOR(S) (Last name, first name, initial) Griffiths, Andrew S.		
6. REPORT DATE 13 January 1972	7a. TOTAL NO. OF PAGES 48	7b. NO. OF REFS 23
8a. CONTRACT OR GRANT NO. F19628-70-C-0230	9a. ORIGINATOR'S REPORT NUMBER(S) Technical Report 490	
b. PROJECT NO. 1508A	9b. OTHER REPORT NO(S) (Any other numbers that may be assigned this report) ESD-TR-72-22	
c.		
d.		
10. AVAILABILITY/LIMITATION NOTICES Approved for public release; distribution unlimited.		
11. SUPPLEMENTARY NOTES None	12. SPONSORING MILITARY ACTIVITY Department of the Navy	
13. ABSTRACT <p>This report describes noise processing experiments with ELF (3 to 300Hz) atmospheric noise and signals in the 40- to 80-Hz range. The primary purpose of the experiments was to design the noise processing portion of a submarine-borne receiver which would minimize the required transmitter power of the Sanguine communications system. The recommended noise processor included a nonlinearity followed by a matched filter and consisted of the following functions: (1) a compensating (or whitening) fiber, (2) a pre-notch filter clipper, (3) notch filters at power line frequencies, (4) a post-notch filter clipper, and (5) a phase-coherent linear matched filter.</p> <p>For nonlinear receivers, an effective noise level (twice the received signal energy divided by the matched filter output signal-to-noise ratio) has been used to measure system performance. Simulations on a digital computer using recorded ELF noise indicate that nonlinear processing provides considerable gain relative to linear processing. For example, using clippers, the highest effective noise levels observed at 45 Hz were about -134, -131, and -137 dB wrt 1 amp/meter $\sqrt{\text{Hz}}$ using Saipan, Malta, and Norway data, respectively, compared to 1 percent exceedance spectral levels of about -115, -115, and -130 dB wrt 1 amp/meter $\sqrt{\text{Hz}}$, respectively.</p> <p>Simulations were conducted to determine the sensitivity of processing gains to several parameters including signal frequency, nonlinearity characteristics, filter characteristics, and platform speed and depth.</p>		
14. KEY WORDS		
nonlinear processing signal processing digital signal processing	noise processing optimal receivers ELF noise	hard limiting hole punching noise clipping